Research Square

Preprints are preliminary reports that have not undergone peer review.
They should not be considered conclusive, used to inform clinical practice,
or referenced by the media as validated information.

A leading genetic cause of short stature in an Arab population

Radwa Sharaf
Dubai Health
Noa Mutsters
University Medical Center Rotterdam
Rawah Mohamed
Dubai Health
Furkan Ozalp
Abdullah Gül University
Ferhan Yenisert
Abdullah Gül University
Sebiha Cevik
Abdullah Gül University
Mohamed Almarri
Mohammed Bin Rashid University of Medicine and Health Sciences
Fatima Taha
Dubai Health
Batool Almoallem
Dubai Health
Tuqa Abdulhameed
Dubai Health
Sarah Alhajjaj
Dubai Health
Maria Farag
Dubai Health
Mahra Fattan
Dubai Health
Rahaf Herzalla
Dubai Health
Dana Obaid
Dubai Health
Tao Zeyuan
Dubai Health
Hamzah Usmani

Dubai Health

Eyad Mustafa
Dubai Health

Ikram Chekroun
Mohammed Bin Rashid University of Medicine and Health Sciences

Ruchi Jain
Dubai Health

Shruti Sinha
Dubai Health

Sathishkumar Ramaswamy
Dubai Health

Maha El-Naofal
Dubai Health

Anju Jacob
Dubai Health

Omer Alkhnbashi
Mohammed Bin Rashid University of Medicine and Health Sciences

Mohamed El-Abiary
Dubai Health

Nandu Thalange
Mohammed Bin Rashid University of Medicine and Health Sciences

Hamad Ali
Kuwait University

Anwar Mohammad
Dasman Diabetes Institute

Alawi A. Alsheikh-Ali
Center for Applied and Translational Genomics (CATG), Mohammed Bin Rashid University of Medicine and Health Sciences, Dubai Health

Patric Delhanty
University Medical Center Rotterdam

Jenny Visser
University Medical Center Rotterdam

Oktay Kaplan
Abdullah Gül University

Ahmad Abou Tayoun
ahmadat@gmail.com

Mohammed Bin Rashid University of Medicine and Health Sciences

Biological Sciences - Article

Keywords:

Posted Date: November 4th, 2026

DOI: https://doi.org/10.21203/rs.3.rs-11608311/v1

License: This work is licensed under a Creative Commons Attribution 4.0 International License.
Read Full License

Additional Declarations: There is **NO** Competing Interest.

A leading genetic cause of short stature in an Arab population

Radwa Sharaf[1], Noa J.M. Mutsters[2], Rawah Mohamed[3], Furkan Ozalp[4], Ferhan Yenisert[4], Sebiha Cevik[4], Mohamed Almarri[5,6], Fatima Taha[3], Batool Almoallem[3], Tuqa Abdulhameed[3], Sarah Alhajjaj[1], Maria Farag[1], Mahra Fattan[1], Rahaf Herzalla[1], Dana Obaid[1], Tao Zeyuan[1], Hamzah Usmani[1], Eyad Mustafa[1], Ikram Chekroun[1], Ruchi Jain[1], Shruti Sinha[1], Sathishkumar Ramaswamy[1], Maha El-Naofal[1], Anju Jacob[3], Omer Alkhnbashi[5], Mohamed El-Abiary[3], Nandu Thalange[5], Hamad Ali[7,8,9], Anwar Mohammad[8], Alawi Alsheikh-Ali[10], Patric J.D. Delhanty[2], Jenny A. Visser[2], Oktay I. Kaplan[4], Ahmad Abou Tayoun[1,5,11,12]

[1]Dubai Health Genomic Medicine Center, Dubai, UAE

[2]Dept of Internal Medicine, Erasmus MC, University Medical Center Rotterdam, Rotterdam, Netherlands

[3]Department of Endocrinology, Al-Jalila Children's Hospital, Dubai Health, Dubai, UAE

[4]Abdullah Gül University, Turkey

[5]College of Medicine, Mohammed Bin Rashid University of Medicine and Health Sciences, Dubai Health, Dubai, UAE

[6]Dubai Police GHQ, Dubai, UAE

[7]Department of Medical Laboratory Sciences, Faculty of Allied Health Sciences, Health Sciences Center, Kuwait University, Jabriya, Kuwait

[8]Translational Research Department, Dasman Diabetes Institute, Dasman, Kuwait

[9]Ministry of Health, Kuwait City, Kuwait

[10]Dubai Health Authority, Dubai, UAE

[11]Center for Genomic Discovery, Dubai Health, Dubai, UAE

[12]Dubai Precision Medicine Center, Dubai Health, Dubai, UAE

Dubai Health - Internal Use

ABSTRACT

Human height is highly heritable and polygenic, yet much of its genetic architecture remains unexplained, especially in underrepresented populations. Here, we analyzed genomic data from 4,862 Middle Eastern patients, including 851 pediatric patients with short stature, and identified a single rare *GHSR* missense variant, p.Arg141Leu, enriched 19-fold in Arab Emirati short stature cases (N=771) vs healthy controls (N=5,151, $P = 1.1 \times 10^{-56}$), explaining 10.2% of Emirati short stature referrals. *GHSR* encodes the ghrelin receptor, and its variants, mostly heterozygous, have previously been linked to short stature. Structural modelling, *in vitro* assays and *Caenorhabditis elegans* studies confirmed loss of function of *GHSR* p.Arg141Leu. Frequent homozygosity and large extended families enabled clinical and biochemical phenotyping of 99 patients across 71 families, revealing semidominant inheritance: homozygotes are more severely affected, and penetrance in heterozygotes is modulated by a polygenic score for height. Both homozygous and heterozygous patients responded to growth hormone therapy. The variant arose through a founder event in the northern United Arab Emirates about 1,700 years ago and is absent from other populations examined. Given its frequency and available treatment, our findings support targeted testing as standard of care in short stature in this population and reveal a hidden contributor to the missing heritability of height.

Dubai Health - Internal Use

INTRODUCTION

Rare diseases pose a significant burden on the population in the Middle East with high rates of consanguinity and founder effects [1–3]. The rapid development and adoption of whole-genome sequencing as a diagnostic tool in pediatric patients has led to the identification of novel genetic causes of rare diseases, particularly in patients from historically underrepresented populations, in some cases being used as a first-line tool [4,5]. Within the region, short stature is one of the most common reasons for genetic testing referrals as poor growth may be a symptom of an underlying genetic condition [6,7]. Differentiating between genetic and non-genetic causes of short stature can have implications on clinical decision-making, determining the necessity and course of treatment [8–10].

Both rare and common genetic variants affect human height concurrently. Genome-wide association studies (GWAS) have identified thousands of independent variants influencing an individual's height, each contributing a small effect, but in aggregate explaining up to 45% of difference in height within a European population [11–13]. Additionally, rare variants with a larger impact on height variability have been observed in patients with short stature. These include mutations in genes within the growth hormone (GH) signaling and regulatory axis, an important pathway in the regulation of linear growth [14,15].

Among these genes, the growth hormone secretagogue receptor (*GHSR*) is of particular interest as it links hypothalamic regulation of energy balance with pituitary GH secretion. *GHSR* encodes a family A G-protein coupled receptor (GPCR), that is highly expressed in the brain and pituitary gland [16,17]. Binding of its ligand, the gut hormone ghrelin, stimulates the release of GH, a major regulator of growth and height [18–21]. The receptor also exhibits significant constitutive activity, amounting to ~50% of its ligand-dependent activity [22,23].

Several heterozygous *GHSR* variants have been studied for their influence on height in both humans [15,24–30] and non-humans [31–33], resulting from either impaired ligand-dependent activity, or constitutive activity, or both, with varying severity and penetrance. However, biallelic disease has rarely been described [24,29,34]. In this study, we analyze genomic data from a large Middle Eastern cohort to investigate a recurrent missense variant in *GHSR*, p.Arg141Leu, among Emirati children with short stature. We characterize the functional effect of the variant using structural modelling, *in vitro* assays and *in vivo* studies in *Caenorhabditis elegans*. Taking advantage of frequent homozygosity and large extended families in this population, we compare heterozygous and homozygous children with intrafamilial controls to define the genotype–phenotype correlation, assess how a height polygenic score influences penetrance, and evaluate patients' response to recombinant human growth hormone (rhGH) treatment. Finally, we examine the origin and population history of the variant and quantify its contribution to genetic short stature in this population.

Dubai Health - Internal Use

RESULTS

Variant observation from internal dataset

At our genomic center, we profiled 4,862 pediatric (<18 years old) patients with rare diseases referred from inpatient and outpatient clinics of varying specialties within the Dubai Health network (companion study). The most frequently identified variant in our rare disease cohort is a single variant of uncertain significance in the *GHSR* gene, NM_198407.2: c.422G>T; p.Arg141Leu, observed in 99 pediatric patients (21 homozygous and 78 heterozygous) from 71 unique nuclear families, referred to genetic testing for short stature.

GHSR variant geographical distribution, founder origin, and association with short stature

We observed a geographical clustering of the variant within the United Arab Emirates (UAE). Families with at least one carrier were concentrated in the northern emirate of Ras Al-Khaimah (43.7%, 31), which is geographically split into two non-contiguous sections (**Figure 1A**), followed by Sharjah (15.5%, 11) and Dubai (12.7%, 9). Of note, 4 families were from neighboring Oman, consistent with the close cultural and geographic ties between the two countries.

Given the geographic concentration of the affected families, we investigated the prevalence of the *GHSR* Arg141Leu variant across large healthy population databases. It was rarely observed in only 2 of 1,614,186 alleles in the Genome Aggregation Database (gnomAD v4.1.1) and in 1 of 1,071,302 alleles in All of Us database (2025 Q4). Thus, we specifically checked prevalence across the Middle East and observed a concentration within the UAE (**Figure 1B**). In a cohort of 5,151 healthy Emirati adults, Arg141Leu was identified in 0.33% of alleles (34/10,302), with no homozygotes found. With the exception of Qatar, where it was observed in 0.024% (3/12,094; 0 homozygotes) of alleles, it was absent from all other Middle Eastern cohorts, including those from Saudi Arabia, Oman, Kuwait, Turkey, as well as from regional databases, including Iranome [58], Almena [59] and DALIA [60]. In Emirati cases referred to genetic testing for short stature (N=771), the variant was observed in 6.2% (95/1,542; 16 homozygotes) of alleles, representing a ~ 19-fold allelic enrichment in cases vs controls (OR 19.8, Fisher's exact $p = 1.1 \times 10^{-56}$, **Figure 1C**). We performed genomic data analysis of six homozygous individuals [61,62], as the ancestral haplotype can be accurately phased, and dated this mutation to 58 generations, or ~1,700 years ago, assuming a generation time of 29 years (**Supplementary Figure 1**). This date is consistent with the variant being a recent, founder mutation confined to Northern UAE.

Gene dose-dependent growth and endocrine phenotype

Dubai Health - Internal Use

We profiled 99 pediatric patients carrying this variant, including one set of monozygotic and one set of dizygotic twins, with a median presentation age of 8 years (**Figure 2, Supplementary Table 1 and 2**). Genomic investigations in patients with the variant included whole-genome (N = 33), whole-exome (N=62), and Sanger sequencing (N=4).

Both homozygotes and heterozygotes demonstrated substantial impairment of linear growth. Median height standard deviation score (SDS) was -3.0 in homozygotes and -2.4 in heterozygotes, significantly lower than either wild-type (WT) siblings from the same families (-0.5) and WT children from other Emirati families (0.1, **Figure 3A**). Short stature (SS), defined as a height of at least 2 SDS below the mean for age and gender, was present in 95.0% (19/20) of homozygotes and 73.7% (56/76) of heterozygotes, consistent with incomplete penetrance in the heterozygous state and a more severe phenotype with biallelic disease. Median deviation from target height was -2.0 for homozygotes and -1.6 for heterozygotes (**Figure 3B**). Growth impairment was not confined to stature. Weight was also reduced for both homozygotes and heterozygotes (median weight SDS -2.9 and -2.5) compared to WT children (1.4, **Figure 3C**). Skeletal maturation was delayed in both groups as well, with median bone-age SDS of -1.6 and -1.3 in homozygotes and heterozygotes, respectively, compared to 0.8 in WT children (**Figure 3D**).

Blood measurements of IGF-1 and IGFBP-3 showed significantly lower levels within both homozygotes (median SDS -2.4 and -2.4) and heterozygotes (-1.7 and -1.4), compared to WT children (-0.2 and -0.5, **Figure 3E-F**). Among patients with growth hormone (GH) stimulation testing results, peak levels were significantly lower in homozygotes vs heterozygotes (median 4.2 and 6.5, p=0.019, **Figure 3G**) and 93.3% (14/15) of homozygotes vs 79.1% (34/43) of heterozygotes met the biochemical criteria for growth hormone deficiency (GHD). Pituitary gland size was assessed by MRI and 83.3% (10/12) of homozygotes had small sizes for their age compared to 62.5% (20/32) of heterozygotes, with a median pituitary gland volume SDS of -1.42 for heterozygotes and -1.65 for homozygotes (**Figure 3H-I**). Consistently across multiple measurements, the phenotype was more pronounced in homozygotes vs heterozygotes (**Figure 3A-H**), whereas all confirmed WT siblings across three families had neither short stature nor a clinical diagnosis of GHD (**Figure 2**).

Among the 93 children in the cohort with self-reported consanguinity status, 52.7% were from consanguineous and 47.3% from non-consanguineous families (**Supplementary Figure 2A**). Homozygosity for the Arg141Leu variant was more common among children of consanguineous vs non-consanguineous unions (17/49, 34.7% vs 3/44, 6.8%; Fisher's exact test p = 0.0011; OR 7.12, **Supplementary Figure 2A**). Genetic data was available for 23 parents and showed that 56.5% of parents (7 fathers and 6 mothers) were heterozygous for the Arg141Leu variant, while 43.5% (4 fathers and 6 mothers) were WT. Of note, none of the

Dubai Health - Internal Use

parents surveyed were homozygous. Parent-of-origin of the *GHSR* variant had no effect on the penetrance of the short stature phenotype (**Supplementary Figure 2B**). We compared the height of parents in this cohort, irrespective of their genotype status, to heights and weights of healthy *GHSR* WT adult Emiratis (**Supplementary Figure 2C-D**). Parents were generally shorter, with a median height SDS of -0.9 for fathers ($p<0.0001$) and -0.7 for mothers ($p<0.0001$, **Supplementary Figure 2E)**. On the other hand, weights of parents in this cohort were comparable to those of healthy Emirati adults, with a median weight SDS of -0.5 for fathers and -0.3 for mothers ($p=0.17$ and 0.28, respectively, **Supplementary Figure 2F**).

Response to treatment

GH treatment was initiated in 59 patients, of which 62.7% (37) were prescribed somatropin (daily dosing) and 37.3% (22) somatrogon (weekly dosing). For some patients, adherence was monitored with Growzen app [35,36] and was above 80% for majority (10/13) of patients (**Supplementary Table 1**). To assess response to GH treatment, we reviewed gains in height in affected children after a median treatment duration of 12.5 months since response within the first year has been shown to predict long-term growth response in children [37]. Median growth velocity was 9.2 cm/year in homozygotes and 8.3 cm/year in heterozygotes, similar to non-*GHSR* patients on GH treatment (8.3 cm/year, **Figure 3J**). Across both genotypes, IGF-1 SDS levels significantly increased compared to pre-treatment levels (**Figure 3K**). Although response to pharmacological GH does not establish endogenous GHD, the observed increase in IGF-1 and linear growth is consistent with preserved peripheral GH responsiveness despite impaired GHSR signaling.

A confounding factor in assessing the response to GH treatment is the presence of an exon 3 deletion in the growth hormone receptor gene (*GHR*), a relatively common allele worldwide and in the Middle East [38,39] and is known to be associated with increased responsiveness to GH regardless of the cause of short stature [40–43]. Overall, there was a similar distribution of the *GHR* exon 3 deletion allele within both *GHSR* Arg141Leu heterozygotes (54%, 13/24) and homozygotes (50%, 5/10). No significant difference was observed in pre-treatment height SDS, post-treatment height SDS, or growth velocity between the *GHR* exon 3 intact and exon 3 deleted allele groups, although overall numbers were small (**Supplementary Figure 3**).

Structural analysis

The recurring missense Arg141Leu variant in *GHSR* lies in the second intracellular loop (ICL2), bordering the third transmembrane domain (TM3, **Supplementary Figure 4A**), specifically within the E/DRY (glutamic/aspartic acid, arginine, tyrosine) motif, a known highly conserved motif across family A GPCRs within various species [44–46] (**Supplementary**

Dubai Health - Internal Use

Figure 4B). Interestingly, arginine, the residue mutated in this variant, is the only invariant residue among all family A GPCRs [47,48]. Computational prediction tools and conservation analyses strongly suggest an impact of Arg141Leu on GHSR protein function (REVEL 0.96 [49] and AlphaGenome Variant Impact 29.7 [50,51]).

To investigate the structural consequences of Arg141Leu variant, we performed 500-ns molecular dynamics simulations of WT and mutant GHSR, with and without ghrelin. The mutation preserved the pre-assembled receptor–Gq complex, where the C-terminal helix (α5) of Gα remained inserted into the cytoplasmic cavity of all four receptors (**Supplementary Figure 4C**). In the presence of ghrelin, the Arg141–Gα Tyr391 hydrogen bond, observed in 47.9% of analyzed frames in WT GHSR, was abolished in the mutant (**Supplementary Figure 4D**), although heavy-atom contact was retained. In the absence of ghrelin, 29 of 56 receptor–Gα contacts changed in the mutant compared to WT by more than 30 percentage points, where α5 remained equally deeply inserted but rotated 21° about its own axis, such that the same residues contacted a different turn of the helix (**Supplementary Figure 4E-G**).

Complete loss-of-function of ghrelin-induced activity

Thus, we characterized the impact of Arg141Leu variant on protein function *in vitro* using HEK293 cells transiently expressing the variant. Compared to WT GHSR, the Arg141Leu variant neither affected total (p=0.09) nor cell surface (p=0.14) protein expression levels (**Figure 5A-B**). We measured calcium mobilization, as a downstream signal of $G\alpha_q$, and observed a complete loss of ghrelin-induced Ca^{2+} response (**Figure 5C**), with an Emax of the fractional response decreasing from 0.29±0.04 for WT GHSR to 0.05±0.02 for the variant receptor (p=0.001, **Figure 5D**). To confirm these results, we measured G protein activity through the dissociation of $G\alpha_q$ from $G\beta_\gamma$ and found a complete loss of $G\alpha_q$ activity (**Figure 5E**), where the Emax decreased from 0.04±0.003 in WT to 0.004±0.003 in Arg141Leu variant (p=0.001, **Figure 5F**), and basal $G\alpha_q$ activity also decreased from 0.02±0.001 to 0.006±0.002 (p=0.003, **Figure 5G**).

To assess the effect of the Arg141Leu variant on $G\alpha_i$ signaling, we measured Serum Response Element (SRE) transcriptional activation as a result of $G\alpha_q$ and $G\alpha_i$ signaling and observed a partial loss of ghrelin-induced SRE response (**Figure 5H**), causing a 40 ± 3.4% reduction in Emax of the SRE response (p=0.007), while basal signaling was not affected (p=0.4, **Figure 5I-J**). To confirm these results, we measured activated GTP bound-$G\alpha_{i2}$ subunits and observed a complete loss of the ghrelin induced $G\alpha_{i2}$ subunit activation for the variant (**Figure 5K**), with the Emax decreasing from 0.015±0.002 in WT to -0.001±0.0007 in Arg141Leu variant (p=0.0008, **Figure 5L**).

Dubai Health - Internal Use

GHSR Arg141Leu behaves as a loss-of-function allele *in vivo*

Since *GHSR* is known to be evolutionary highly conserved [21,52–56], we generated an animal model of the Arg141Leu variant to characterize its *in vivo* role. In *C. elegans*, K03H6.5 encodes a family A GPCR, identified as a likely ortholog of mammalian *GHSR*, but has not been experimentally studied [57]. We therefore characterized a K03H6.5 homozygous knockout strain (tm4483, referred to as null) and a humanized homozygous Arg141Leu mutant strain generated by CRISPR/Cas9 (Methods).

To assess the impact of both mutations on the growth and size of worms, we performed a developmental growth analysis evaluating post-embryonic growth, from the L1 larval stage (15 hours post-hatching) through 1-day adulthood (101 hours post-hatching) within each strain. A consistent and statistically significant reduction in body length was observed in both the null and Arg141Leu strains compared with WT at L4 (median body length in μm for WT, null, Arg141Leu: 547.5, 501.3, 480.4) and at 1-day adult stages (654.1, 619.7, 620.1, **Figure 6**). Interestingly, Arg141Leu showed a slightly stronger reduction in body length than the null allele during the early larval stages (L1, p=0.006) and (L2, p=0.0002). However, by the L4 and 1-day adult stages, Arg141Leu essentially phenocopied the null allele *in vivo* (p = 0.14 at L4; p=0.69 at 1-day adult). Both the null and Arg141Leu strains responded well to gentle touch, similar to WT, with a response recorded in all animals (40/40) within each genotype. Finally, we assessed the neuronal health of the worms to check for uncoordinated movement. The tracking assay showed that both mutants displayed tracks comparable to WT (**Supplementary Figure 5**).

Height polygenic score

Since height is a polygenic trait influenced by numerous genetic variants, we assessed the impact of a height polygenic score (PGS) on penetrance of the Arg141Leu variant. Within a healthy Emirati adult cohort with confirmed WT *GHSR* status and available height data (N=1919), we tested PGS002802, a height polygenic score generated from the largest height GWAS published to-date, but this accounted for only 6.5% of total variance in height in our cohort (β= 0.25, p<0.0001, R^2 = 0.065, **Supplementary Figure 6A**). Thus, we tested eight published height score models from the PGS Catalog (GRCh38-harmonised, computed from WGS) [11,12] and performance of each was evaluated by 10-fold cross-validation (out-of-fold R^2). The best-performing model (PGS004782) was an ensemble approach, originally trained on South Asians and explained 17.2% of height SDS variance in our healthy Emirati adult population cohort (**Supplementary Figure 6A**). PGS004782 was then validated in *GHSR* WT children (N = 385), where a low PGS was associated with shorter stature, as expected (**Supplementary Figure 6B**).

Dubai Health - Internal Use

Subsequently, we applied it to WGS-profiled pediatric patients, harboring the *GHSR* Arg141Leu variant (20 heterozygotes, 9 homozygotes). We observed that the PGS score influenced the penetrance of the *GHSR* variant in the heterozygous state (**Figure 6A**). Using a height SDS threshold of -2 to define short stature, penetrance of the short stature phenotype in heterozygotes with high PGS was 25% only, compared to 93.8% in heterozygotes with low PGS (p=0.0134, **Figure 6A**). For homozygotes, penetrance was 100% within both groups.

Evidence for variant reclassification

The case enrichment, along with the functional *in vitro* and *in vivo* data, prompted the reclassification of *GHSR* Arg141Leu from uncertain to pathogenic (**Supplementary Table 3**), more than doubling the diagnostic yield of Emirati pediatric short stature cases, increasing from 6.1% (47/771) to 16.3% (126/771, **Figure 6B**). This single variant accounted for 62.7% of positive cases, explaining 10.2% (79/771) of all Emirati short stature referrals, representing an allelic frequency of 6.2% (95/1542) in Emirati cases.

Dubai Health - Internal Use

DISCUSSION

Short stature (defined as a height less than 2 standard deviation score below the mean for matched age and gender) is one of the most common reasons for referral to pediatric endocrinology, accounting for approximately 50% of new visits [7,63,64]. Positive diagnostic yield for children referred for genetic testing due to short stature is generally low, with a monogenic cause identified in 8.8%-15% of children with isolated short stature and in up to 51% of children with syndromic short stature [65–70]. Within our cohort, short stature accounted for 17.5% of pediatric patient referrals to genetic testing. A single variant, *GHSR* Arg141Leu, explained 10.2% of Emirati short stature cases and was the most frequently reported variant amongst the entire rare disease pediatric patient cohort (N=4,862), irrespective of clinical indication or nationality.

Previous studies have linked loss-of-function *GHSR* variants with familial short stature and growth hormone deficiency with varying severity [15,24,25,29,30]. The *GHSR* short-stature literature primarily focuses on heterozygous *GHSR* variants, including the largest cohort study to-date, which included 26 heterozygous patients [15,25,26,71–73]. Only a handful of case reports on homozygous or compound heterozygous variants were published, describing one patient each [24,29,34].

The size of our cohort and availability of individuals across both genotype states (21 homozygotes and 78 heterozygotes) provide an opportunity to refine the endocrine phenotype associated with impaired GHSR signaling. Affected children demonstrated not only short stature, but a broader pattern comprising reduced weight, delayed skeletal maturation, low IGF-1 concentrations, smaller pituitary gland size, and subnormal GH responses to pharmacological stimulation. Because GHSR itself participates in physiological regulation of GH secretion, these findings represent subnormal stimulated GH responses rather than conventional pituitary GH deficiency. The generally greater impairment observed in homozygotes supports a gene-dose effect and is consistent with semidominant inheritance. Peripheral response to GH treatment within these patients remains preserved, with the defect largely operating upstream of GH action.

Mechanistically, GHSR primarily couples to $G\alpha_q$/PLC, mobilizing intracellular Ca^{2+} via IP3 and can signal through alternate pathways including $G\alpha_i$ [16,22,74,75]. The variant results in a change of the arginine residue in the E/DRY motif of GHSR. As a basic amino acid, arginine forms stable interactions with the adjacent glutamic/aspartic acid residue, critical for the transfer of an activating signal from the receptor to the G-protein, activating the rate-limiting step of GDP release from the G-protein α subunit and further downstream signal transduction [76,77]. In addition, neutralization of the salt bridge created between the arginine in E/DRY motif and a partially conserved glutamic acid of transmembrane helix 6 is a crucial

Dubai Health - Internal Use

early step in receptor activation, shifting to the active conformation [78–80]. Substitutions of this arginine to different basic or non-basic amino acids across various GPCRs led to reduced G-protein coupling or improper receptor folding and trafficking, resulting in a decrease in signal transduction [45,76,81–92], with only two reports showing preserved receptor activity upon substitution to other basic amino acids in some GPCRs [93,94].

Specifically, arginine-to-leucine substitutions in the E/DRY motif of most GPCRs, including Rhodopsin, resulted in a decrease of *in vitro* activity [82,95–98] and disease [99,100]. However, in one GPCR (V2R), the same substitution led to a constitutively active receptor and was described in a patient with inappropriate antidiuretic hormone secretion syndrome [101]. In *GHSR*, Arg141Leu has not been previously described, except for a historical descriptive cohort analysis from our genomic center listing one heterozygous patient with growth failure harboring this variant [1].

A different amino acid change in *GHSR* at the same position (Arg141Pro) was recently identified in a heterozygous state in 6 patients with short stature and was shown to suppress both ligand-dependent and -independent receptor activity *in vitro*, as well as markedly reduce cell surface expression [15]. Even though proline (Arg141Pro, previously described) and leucine (Arg141Leu, described here) are both hydrophobic, their structures differ significantly, where proline has a rigid cyclic ring and leucine a flexible side chain.

Our *in vitro* functional characterization establishes causality of the Arg141Leu variant, displaying preserved cell surface expression but abrogated signaling via both $G\alpha_q$ and $G\alpha_i$ and simulations provide a structural rationale for the loss of function. *GHSR* is known to be evolutionary conserved among vertebrate species [21,52–56]. We used body length in *C. elegans* as a quantitative *in vivo* readout of receptor function, which allowed us to compare the Arg141Leu knock-in allele directly against a deletion allele of the same gene in an intact animal. We demonstrated that *GHSR* Arg141Leu behaved like a complete knockout in the worms, leading to shorter body lengths.

The variant was observed in 3 total alleles across both gnomAD and All of Us, with no homozygotes identified in either database. The strong geographic concentration within the UAE, and specifically within the northern Emirate of Ras Al-Khaimah, in addition to the variant dating evidence from studying shared ancestral haplotypes, is strongly suggestive of this variant being a founder mutation in the Emirati population. From an evolutionary perspective, shorter smaller bodies have less nutritional requirements, which could have been an advantage in a food-scarce desert setting [102]. Over the last 50 years, the UAE has experienced rapid urbanization and economic growth. Emirati children heights have shown a significant increase between 1992 and 2021, attributed to better nutrition and improved

Dubai Health - Internal Use

healthcare [103,104], a setting where the variant may not be expected to have an evolutionary advantage, yet it persists.

Previous studies have documented an effect of parent-of-origin of variants on the height of children [105–107], but in our cohort, we did not observe a difference on the penetrance of the short stature phenotype. Interestingly, some heterozygotes did not suffer from short stature. For a highly polygenic trait such as height, the phenotypic effect of a single variant may be attenuated by the cumulative contribution of multiple additional genetic variants influencing stature [108,109]. Our data showed that the height polygenic score modified phenotypic expression in heterozygotes, illustrating the interaction between a rare variant of relatively large functional effect and the polygenic architecture of human height. In homozygotes, the effect of biallelic receptor dysfunction appears to reduce the modifying influence of polygenic background.

Our work has some limitations. Five pediatric patients (5.1%) were diagnosed with other conditions that could provide an alternative explanation for the observed short stature and growth failure, including skeletal dysplasia, Turner syndrome, inflammatory bowel disease, celiac disease, and chronic kidney disease. However, in most patients, no other conditions were diagnosed and a sensitivity analysis excluding these patients retained the statistically significant differences in height, IGF-1 and IGFBP3 standard deviation scores across groups. Some of our analyses, including variant dating and polygenic scoring, were limited to samples sequenced by WGS, representing only a subset of the total cohort. A larger WGS cohort size can further corroborate our findings.

Endocrine phenotyping was retrospective and not all measurements were available in all participants. In addition, we utilized GH stimulation testing for the diagnosis of GHD, since it remains to be the gold standard, however stimulation testing has low specificity and reproducibility, substantial intra-individual variability and diagnostic thresholds that vary between centers and stimulating agents [9,110–113]. Thus, the interpretation of results in this setting requires caution. In cases when a GHD diagnosis is established, GH treatment is initiated. Treatment response is influenced by multiple factors, including the child's age, weight, difference of their height from the mid-parental height, treatment duration, dose, and adherence [114–117]. Adherence was evaluated in a subset of patients and was found to be generally high; however a larger cohort size adjusted for these covariates can further strengthen our results.

Notwithstanding these limitations, our work has several wide implications. The fact that such a common cause of genetic stature in this population has been overlooked emphasizes the continuous bias in genomic studies towards European ancestries and the underrepresentation of other populations in healthy and disease databases. This work also

Dubai Health - Internal Use

highlights how founder effects, consanguinity, and large pedigrees, characteristic of the Middle Eastern populations, are crucial genetic tools that can enhance our understanding of genetic diseases, their inheritance, penetrance, polygenic interaction, as well as the underlying human biology.

Since this mutation impacts the conserved E/DRY motif, we hypothesize that arginine-to-leucine substitutions across various GPCRs harboring this motif would similarly have severe effects. This would potentially have wide implications since GPCRs constitute the largest group of membrane proteins, with 805 unique GPCR proteins listed in GPCRdb, and specifically family A being the largest (~700 proteins) [46,118–121]. Furthermore, GPCRs constitute an estimated 15-35% of all current approved drug targets, representing the largest group [121–125]. Despite this, only a small fraction (~15%) of GPCRs are targets of approved drugs, suggesting an untapped potential for a molecule that can rescue activity of variants, presumably across other disease-relevant family A GPCRs, including Arg141Leu.

Acknowledgments

We thank the study participants for their contributions, as well as Fowzan Alkuraya, Khalid Fakhro, Fahd Al Mulla, Uğur Özbek, and Almundher Al-Maawali for querying their internal cohorts.

Data availability

All underlying data used to generate Figures 1A, 2, 3 and Supplementary Figures 2 and 3 are available in Supplementary Table 1 and 2.

Dubai Health - Internal Use

Figure legends

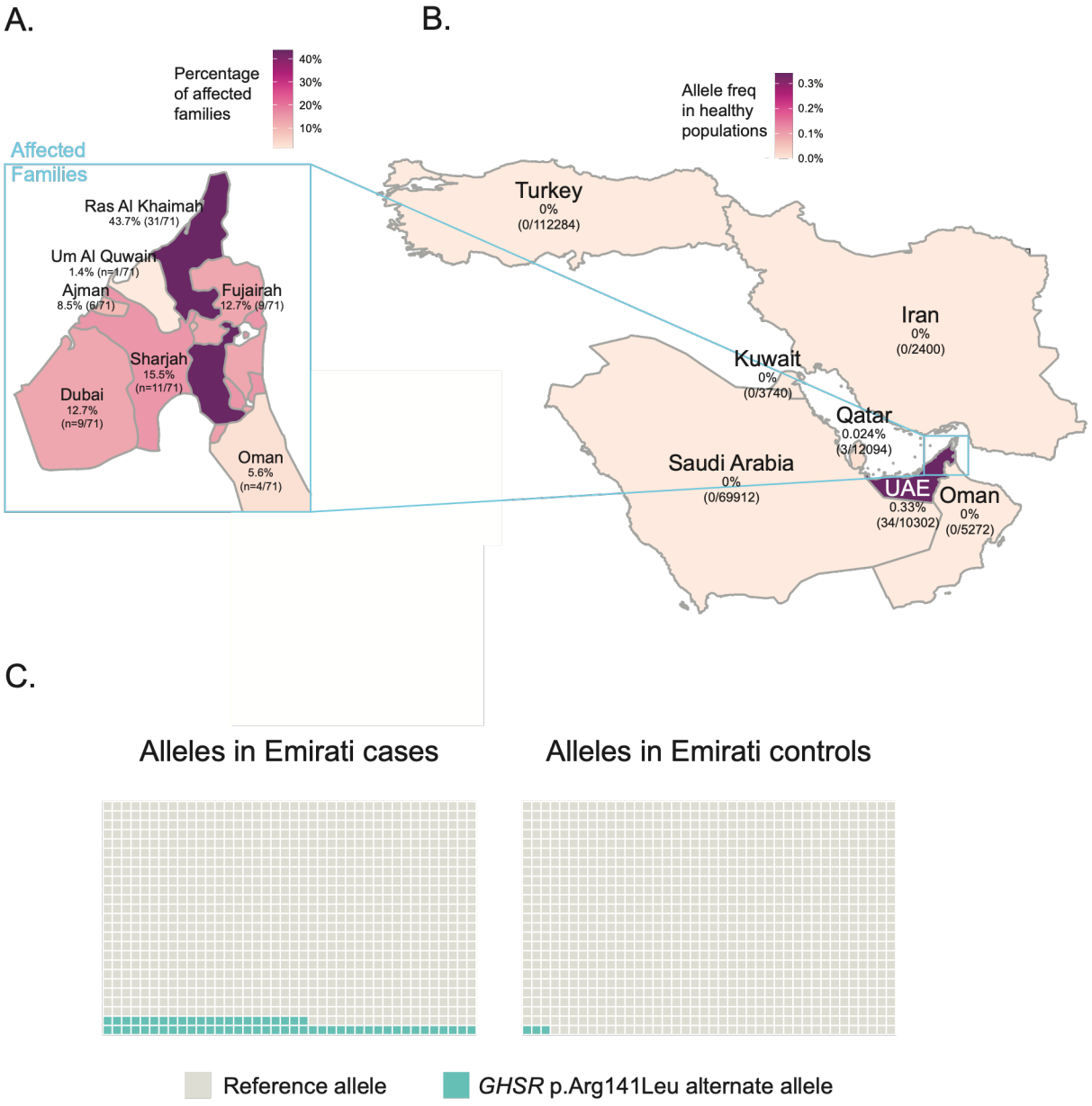


Figure 1. *GHSR* Arg141Leu geographic distribution and case-control enrichment analysis. A. Geographic distribution of families with affected children across the UAE, with each Emirate shaded according to the percentage of affected families originating from it. **B.** Geographic distribution of healthy Arg141Leu carriers across the Middle East, with each country shaded according to allele frequency. freq, frequency. **C.** Waffle plot depicting *GHSR* p.Arg141Leu allele fraction in Emirati short-stature cases (N=1542) and population controls (N=10,302). Teal squares denote the p.Arg141Leu allele and grey squares are the reference

allele. Each square represents 0.1% of its group's alleles. In cases, one square is equivalent to 1.5 alleles and in controls 10.3 alleles. Values are rounded to the nearest whole square.

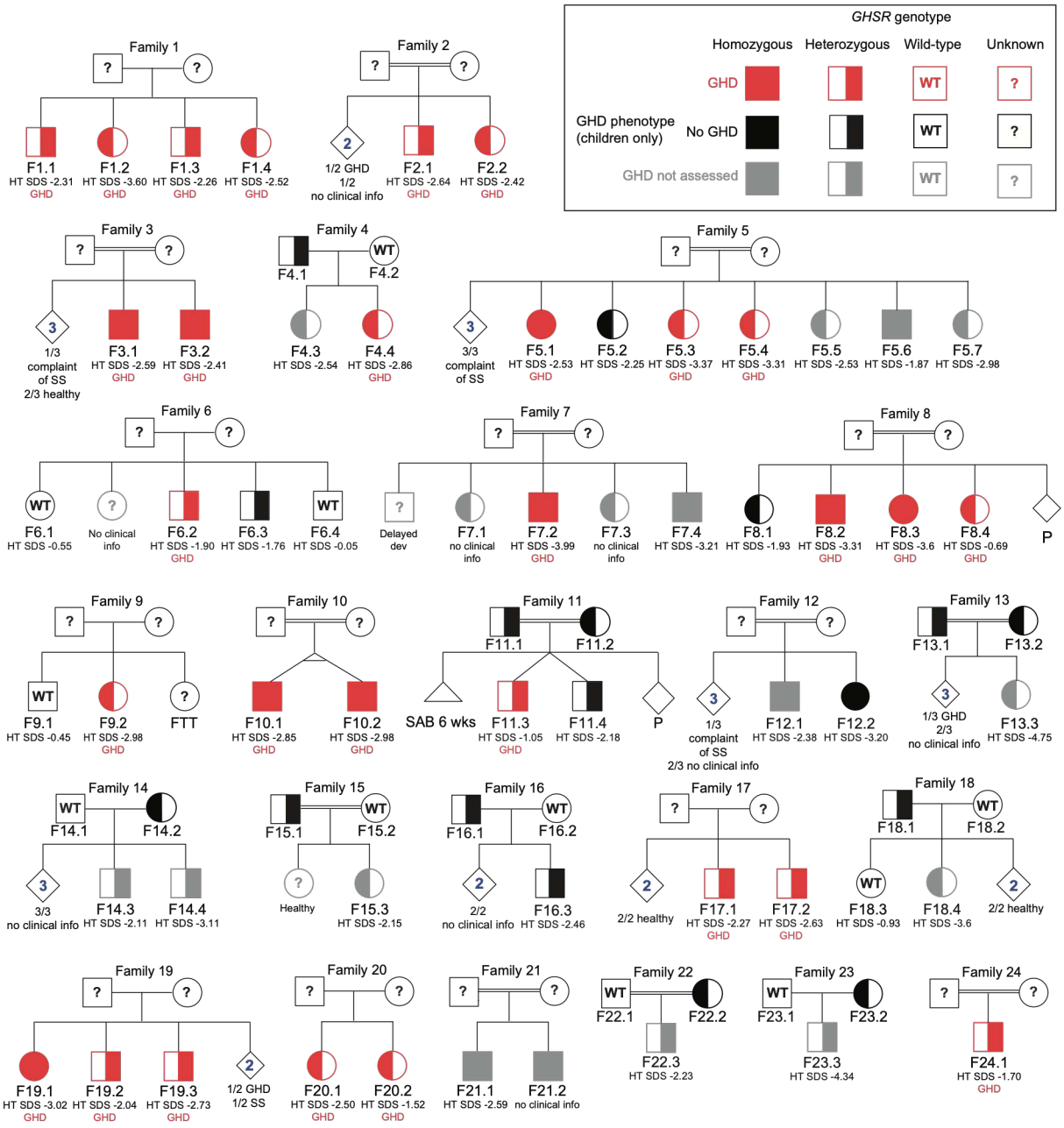


Figure 2. *GHSR* family pedigrees. Individuals with completely filled symbols are homozygous for the variant, half-filled are heterozygous, unfilled symbols labelled "WT" are wild-type, and symbols marked with a question mark indicate untested individuals. Diamonds indicate siblings, with the number of siblings shown inside the diamond and available clinical information shown underneath. The presence or absence of growth hormone deficiency (GHD) in the children is indicated by red color shading. The height

Dubai Health - Internal Use

standard deviation score (HT SDS) is shown beneath each individual. A double horizontal line indicates a consanguineous couple. Twins are drawn as two diagonal lines from a single point, with an additional horizontal connecting line for identical twins. Delayed dev, delayed development; P, pregnant; SAB, spontaneous abortion; SS, short stature.

Dubai Health - Internal Use

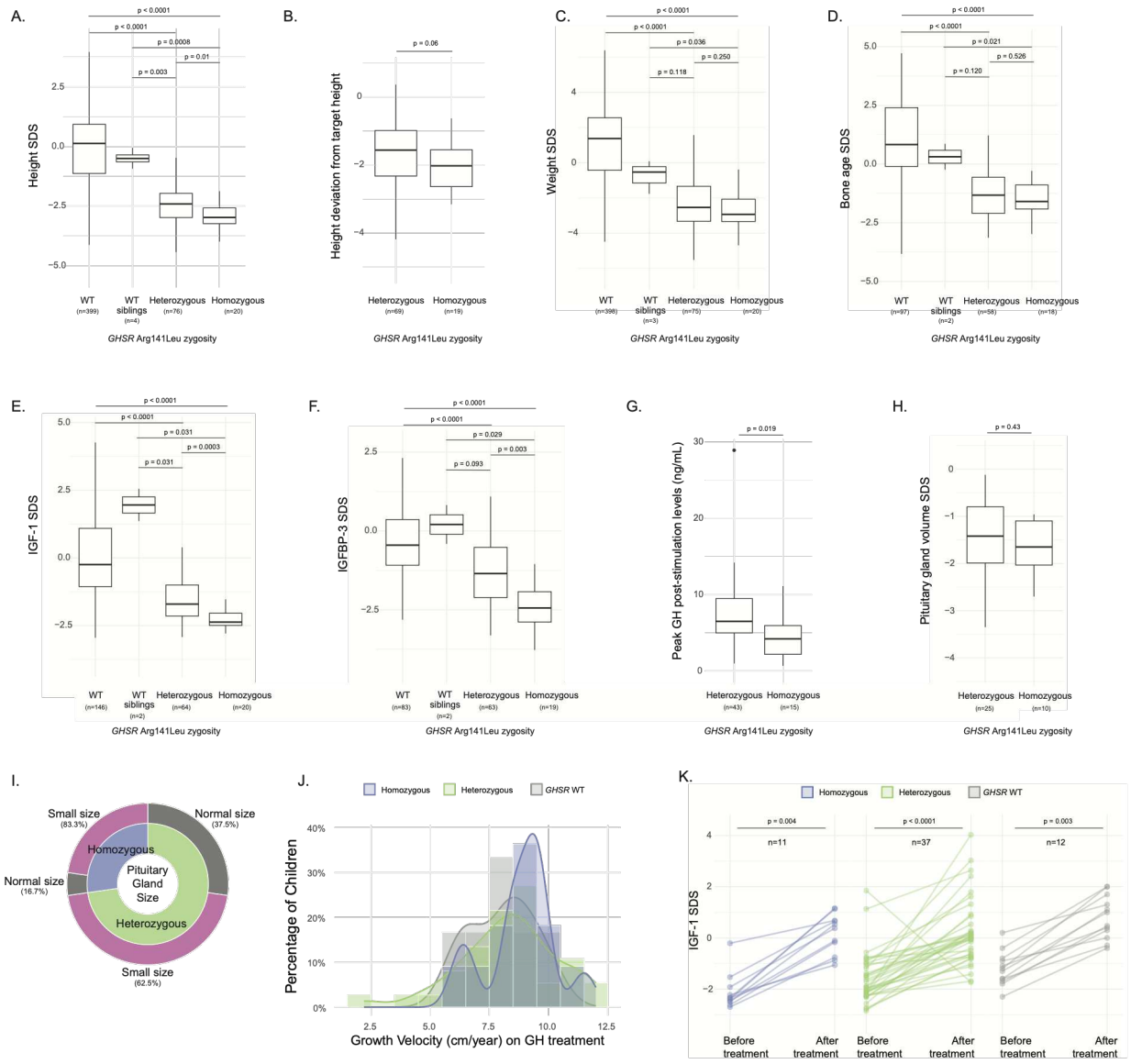


Figure 3. Clinical and biochemical characteristics of patients and controls. Boxplots of height SDS (**A**), height deviation from target height (**B**), weight SDS (**C**), bone age SDS (**D**), blood IGF-1 levels (**E**) and blood IGFBP-3 levels (**F**) for WT, heterozygous, and homozygous pediatric patients are depicted. **G**. Peak GH levels after arginine stimulation for heterozygous and homozygous patients. **H**. Pituitary gland volume SDS as assessed by MRI imaging. Statistical testing for A-H was performed using pairwise Wilcoxon rank sum tests with Benjamini–Hochberg correction. **I**. Qualitative assessment by radiologist of pituitary gland size for patient's age. Within each panel (A-I), patient counts may differ due to incomplete patient records. **J**. Smoothed histogram of growth velocity (cm/year) in response to GH treatment. **K**. Line plot displaying blood IGF-1 levels before and after recombinant human GH treatment. Pre- vs post-treatment IGF1 SDS levels were compared using Wilcoxon signed-rank test for paired samples.

Dubai Health - Internal Use

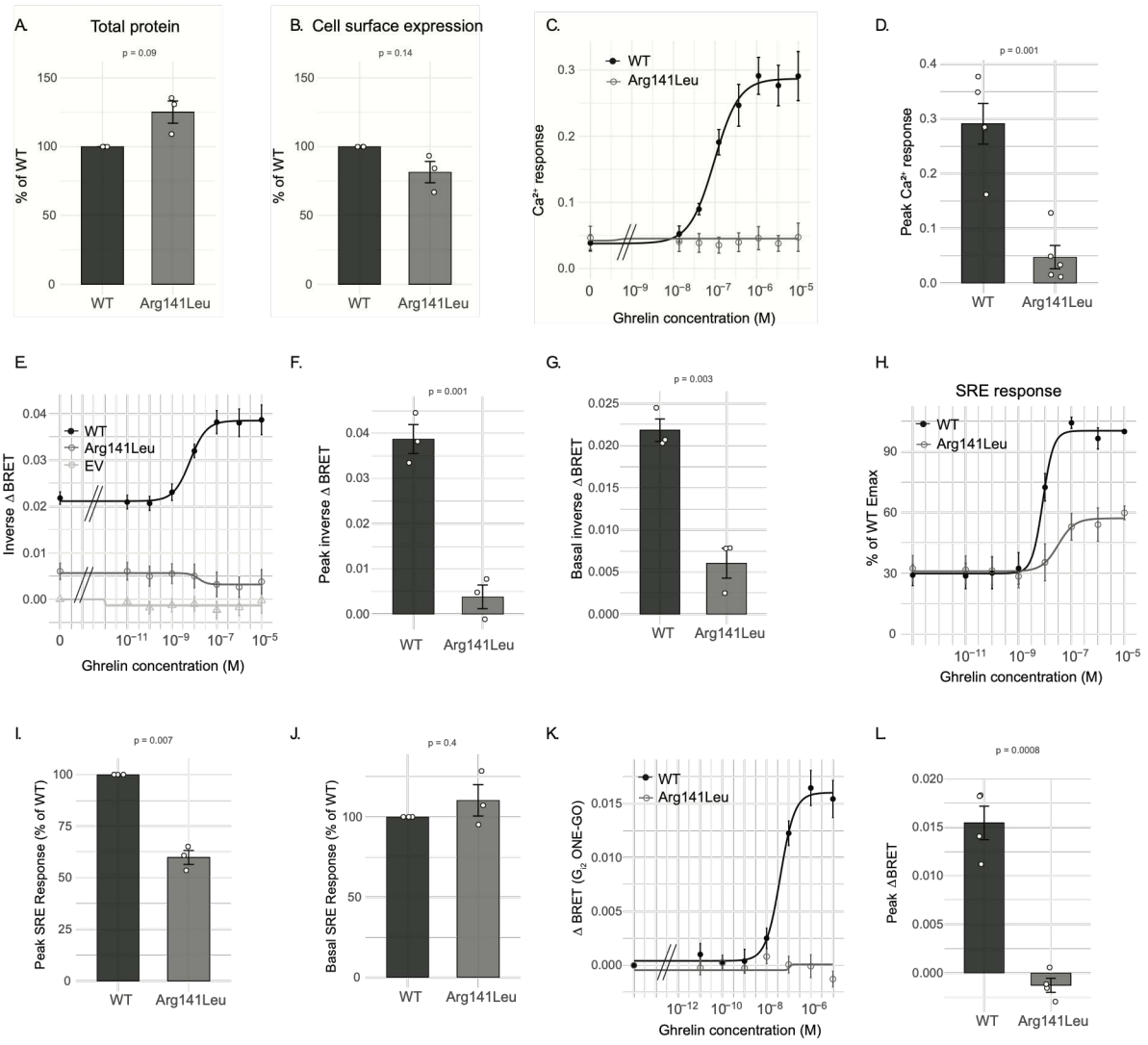


Figure 4. *In vitro* effect of the Arg141Leu on GHSR G-protein coupled receptor signaling. Bar plot of total protein (**A**) and cell surface (**B**) expression levels in cells transfected with GHSR Arg141Leu, compared to wild type GHSR. Dose-response curve (**C**) and peak activity (**D**) of ghrelin-induced Ca^{2+} response. Dose-response curve (**E**), peak (**F**), and basal (**G**) response of ghrelin-induced $G\alpha_q$ activity. Dose-response curve (**H**), peak (**I**), and basal (**J**) response of ghrelin-induced SRE activity. Dose-response curve (**K**) and peak (**L**) response of ghrelin-induced $G\alpha_{i2}$ subunit activation. EV, empty vector. Welch's t-test was used for comparison between WT and Arg141Leu.

Dubai Health - Internal Use

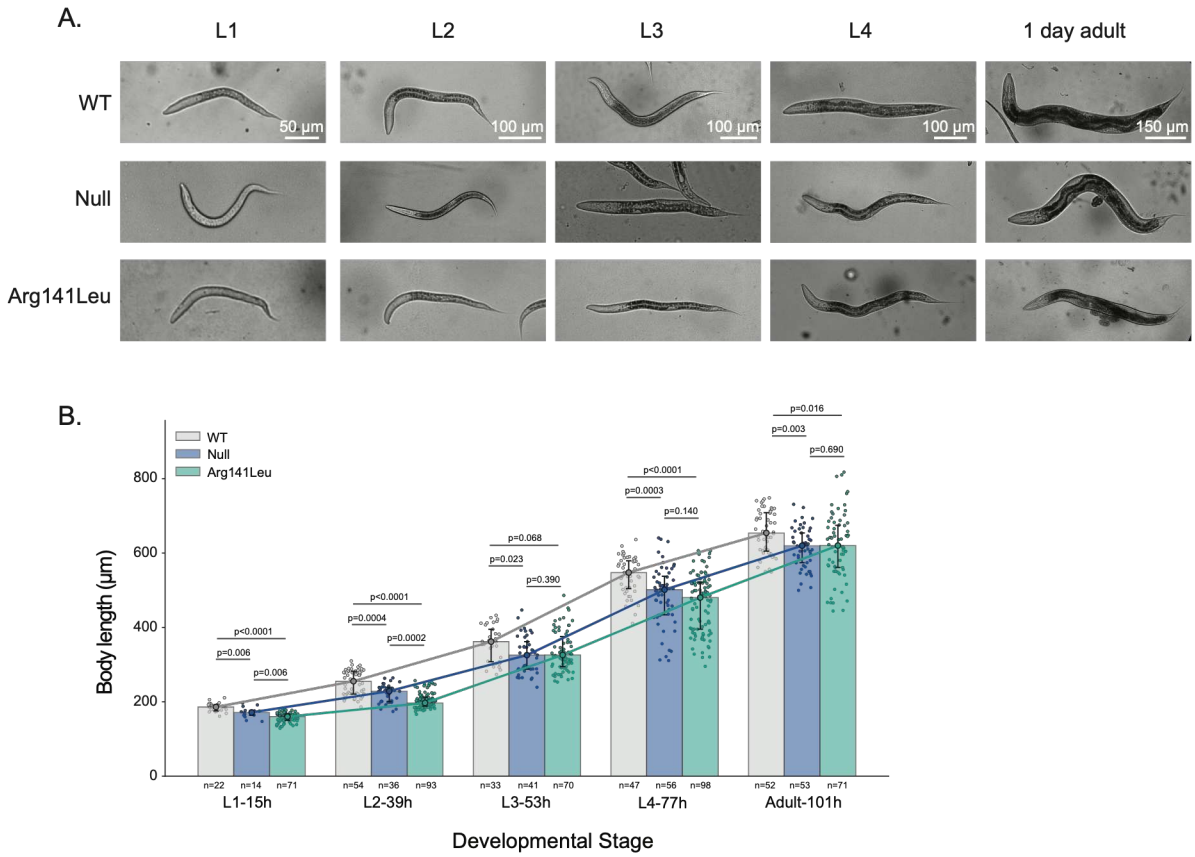


Figure 5. *In vivo* effect of the Arg141Leu on body length in a *C. elegans* animal model. A. Representative brightfield images of WT, null, and Arg141Leu *C. elegans* at the indicated developmental stages. **B.** Body length measurements of WT, null, and Arg141Leu *C. elegans* strains throughout development, from early larval stages (L1 and L2) till 1-day adult stage. Individual animals are shown as points, with lines connecting the mean body length at each developmental stage. Statistical testing was performed using pairwise Wilcoxon rank sum tests with Benjamini–Hochberg correction.

Dubai Health - Internal Use

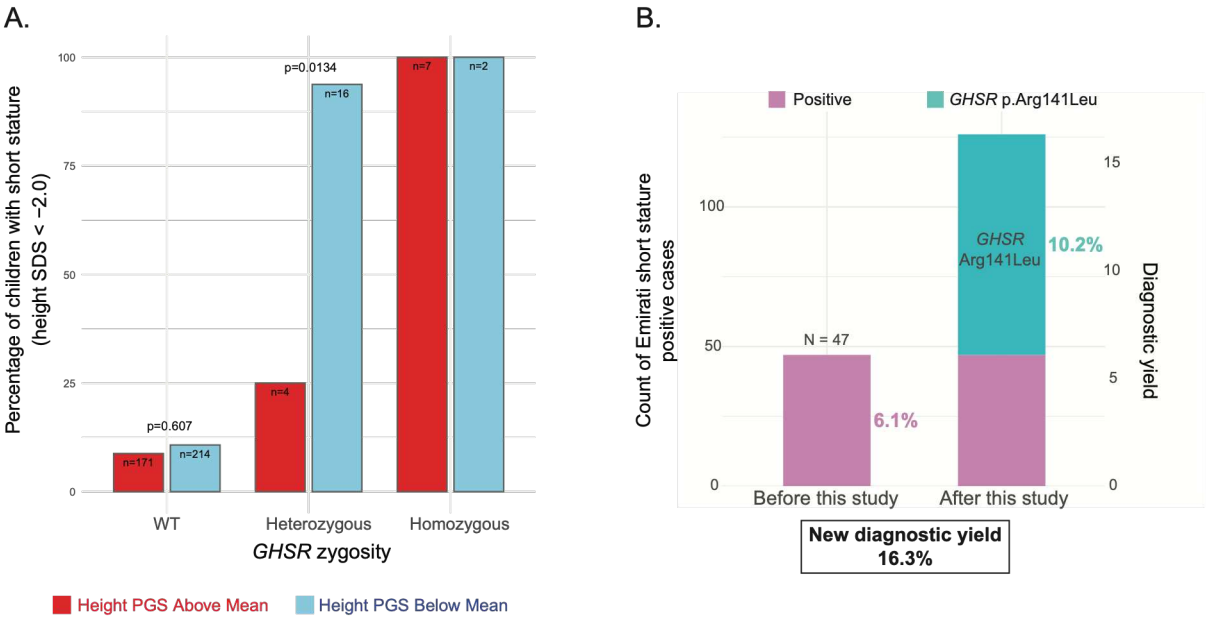
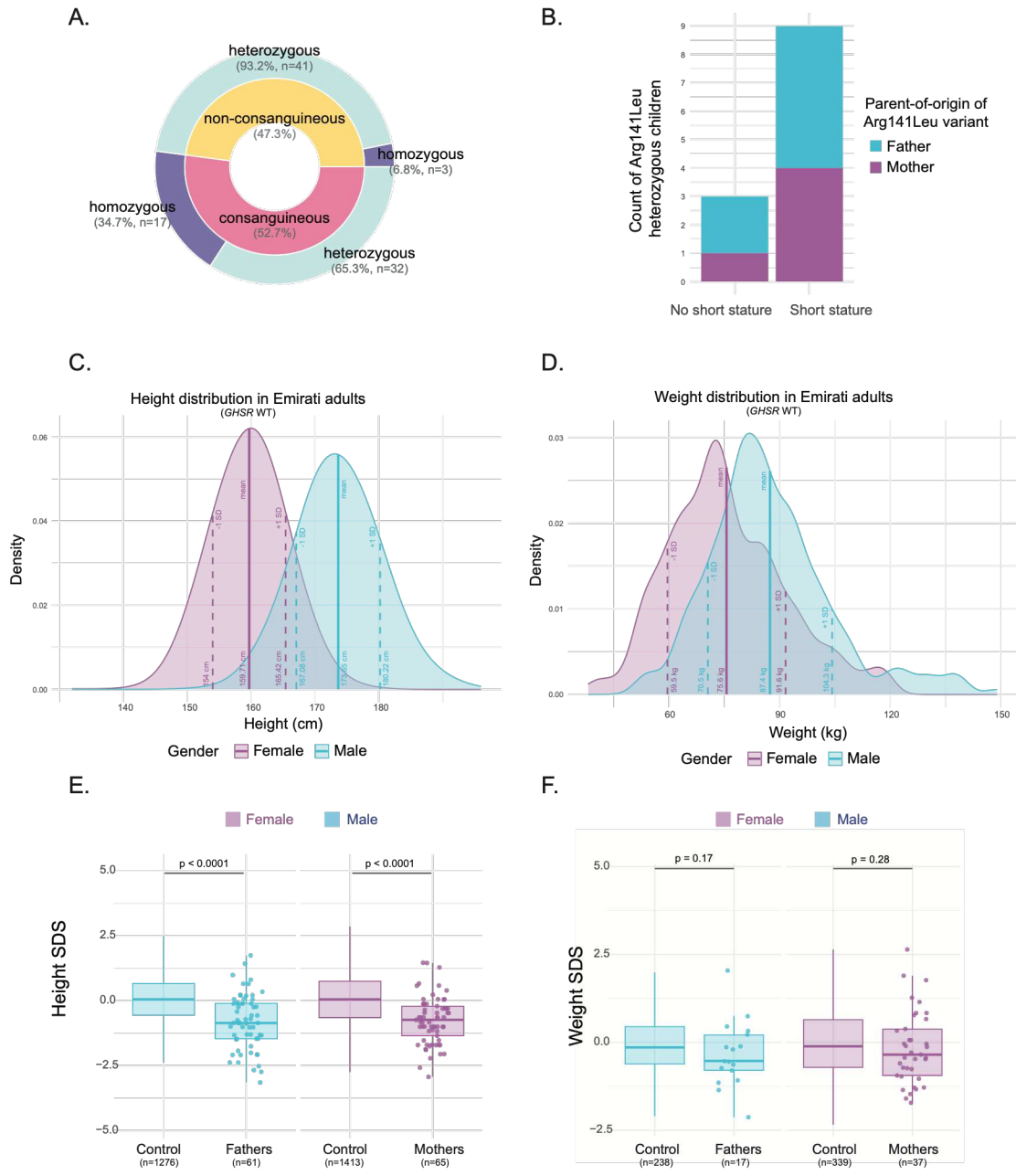


Figure 6. *GHSR* Arg141Leu case-control enrichment analysis, its interaction with height polygenic score, and geographic distribution. A. Proportion of children with short stature, defined as height below 2 SDS, stratified by height polygenic score grouping and variant zygosity. **B.** Diagnostic yield in Emirati pediatric short stature cases tested by whole-exome or whole-genome sequencing, before (6.1%) and after this study (16.3%), which led to Arg141Leu reclassification to pathogenic. Each patient is counted once.



Supplementary Figure 1. Shared ancestral haplotype surrounding the NM_198407.2 c.422G>T variant, corresponding to chr3:172,447,992 C>A (GRCh38) on the negative strand, across six homozygous individuals. The upper axis and lower axis display the genetic and physical distance from the mutation in centimorgans (cM) and megabases (Mb), respectively. Colored segments indicate, for each informative marker, whether that individual's haplotype is concordant and shared with the other carrier haplotypes (dark blue), discordant as the opposite homozygote (dark red), or discordant but heterozygous (yellow). The called shared identity-by-descent (IBD) segment is marked by a black line. CI, confidence interval.

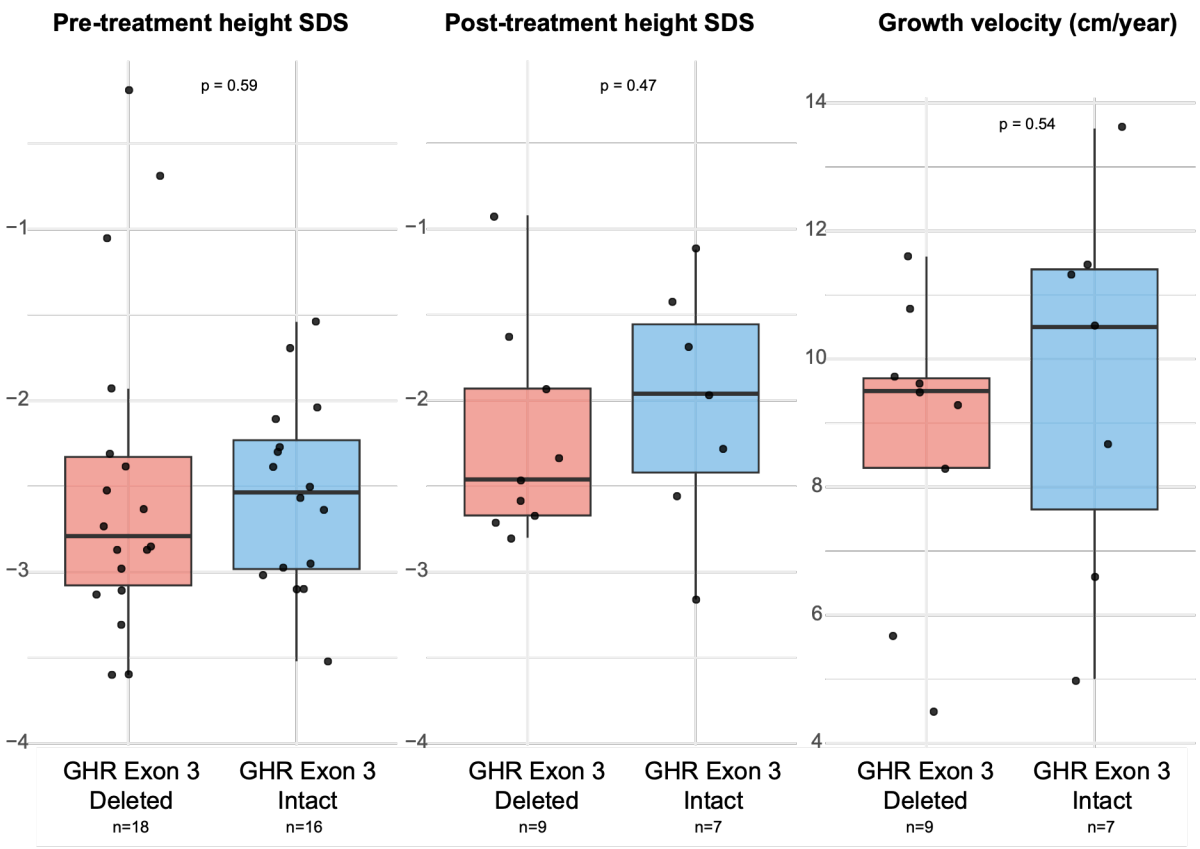
Dubai Health - Internal Use



Supplementary Figure 2. Distribution of consanguinity and variant parent-of-origin among patients, along with height and weight distribution among their parents. A. Donut plot displaying distribution of consanguinity and variant zygosity among pediatric patients. **B**. Stacked barplot depicting parent-of-origin of the *GHSR* Arg141Leu variant in heterozygous children with or without clinically-defined short stature. Height (**C**) and weight (**D**) distribution of healthy adult Emiratis with confirmed *GHSR* WT status. Data for females and males are color-coded in pink and blue, respectively. The thick solid line indicates the mean, while the dotted lines represent ±1 standard deviation (SD). Boxplot of height SDS (**E**) and weight SDS (**F**) for parents of pediatric patients vs healthy adult Emirati controls, split by

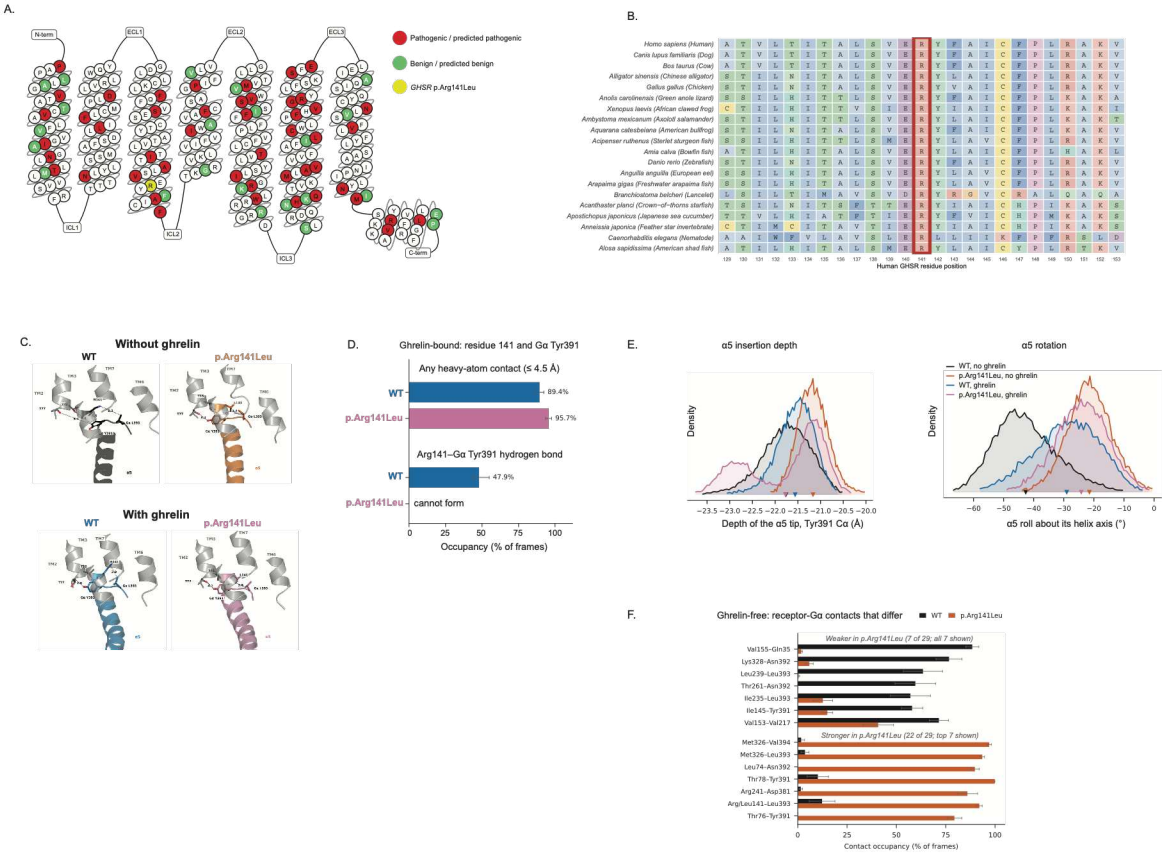
Dubai Health - Internal Use

gender. Two-sided Wilcoxon rank-sum test was used to compare parent vs control height SDS.



Supplementary Figure 3. Effect of growth hormone receptor (*GHR*) exon 3 deletion on *GHSR* patients' response to treatment. Boxplot comparing pre-treatment height SDS, post-treatment height SDS, and growth velocity (cm/year) between GHR exon3-deleted and GHR exon3-intact.

Dubai Health - Internal Use

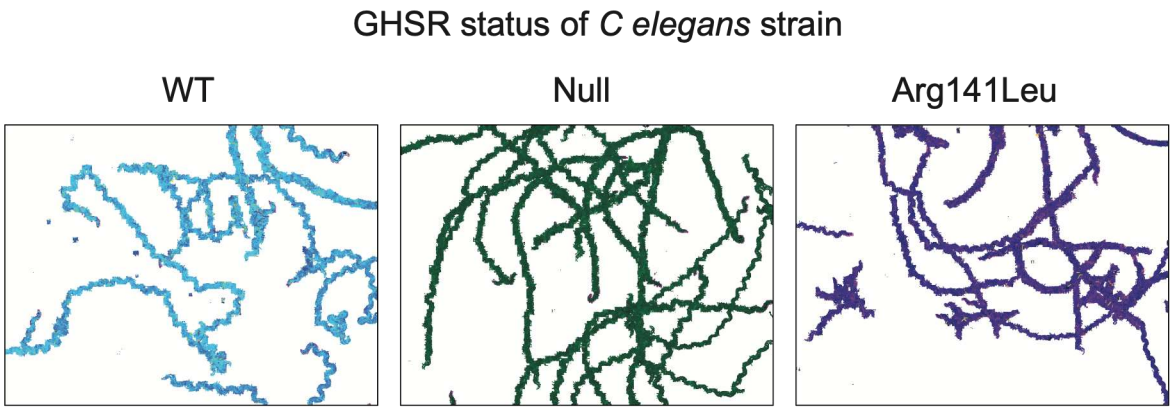


Supplementary Figure 4. GHSR protein structure and conservation across species. A. Snake-plot of documented genetic variants within *GHSR* with predicted/confirmed status in red (pathogenic) or green (benign). Arg141Leu is highlighted in yellow. Created by gpcrdb.org. ECL, extracellular loop; ICL, intracellular loop. **B.** Multi-sequence alignment of the region surrounding *GHSR* E/DRY motif across diverse species. **C.** Representative frames from the 500 ns simulations of WT and Arg141Leu GHSR–Gq complexes without (top) and with (bottom) ghrelin, each the frame closest to the window-average structure of the receptor transmembrane helices and α5. Receptor helices are gray and the Gα α5 helix is colored by system; residue 141, Thr77, Thr78, Gα Tyr391 and Gα Leu393 are shown with the closest heavy-atom distance in that frame. TM, transmembrane. **D.** Residue 141 against Gα Tyr391 in the ghrelin-bound systems: heavy-atom contact is retained in the variant (89.4% in WT, 95.7% in Arg141Leu), whereas the Arg141 side-chain hydrogen bond to the Tyr391 backbone carbonyl, present in 47.9% of WT frames, cannot form with leucine. **E.** Left: Distribution of α5 roll about its own helix axis over the analysis window, measured in a receptor frame fitted on the transmembrane helices and referenced to the deposited ghrelin-bound complex; markers under each curve are the window means. Right: Depth of the α5 tip (Tyr391 Cα) over the same frames. **F.** Receptor–Gα contacts in the ghrelin-free systems. Of the 56 pairs present in at least half the frames of either system, 29 differ by more than 30 percentage points: 22 strengthen in the variant and 7 weaken. All seven weakened pairs are shown together with the seven strongest gains. Occupancies are percentages of frames over 200–500 ns and contacts are defined by a closest heavy-atom distance of 4.5 Å or less; error bars

Dubai Health - Internal Use

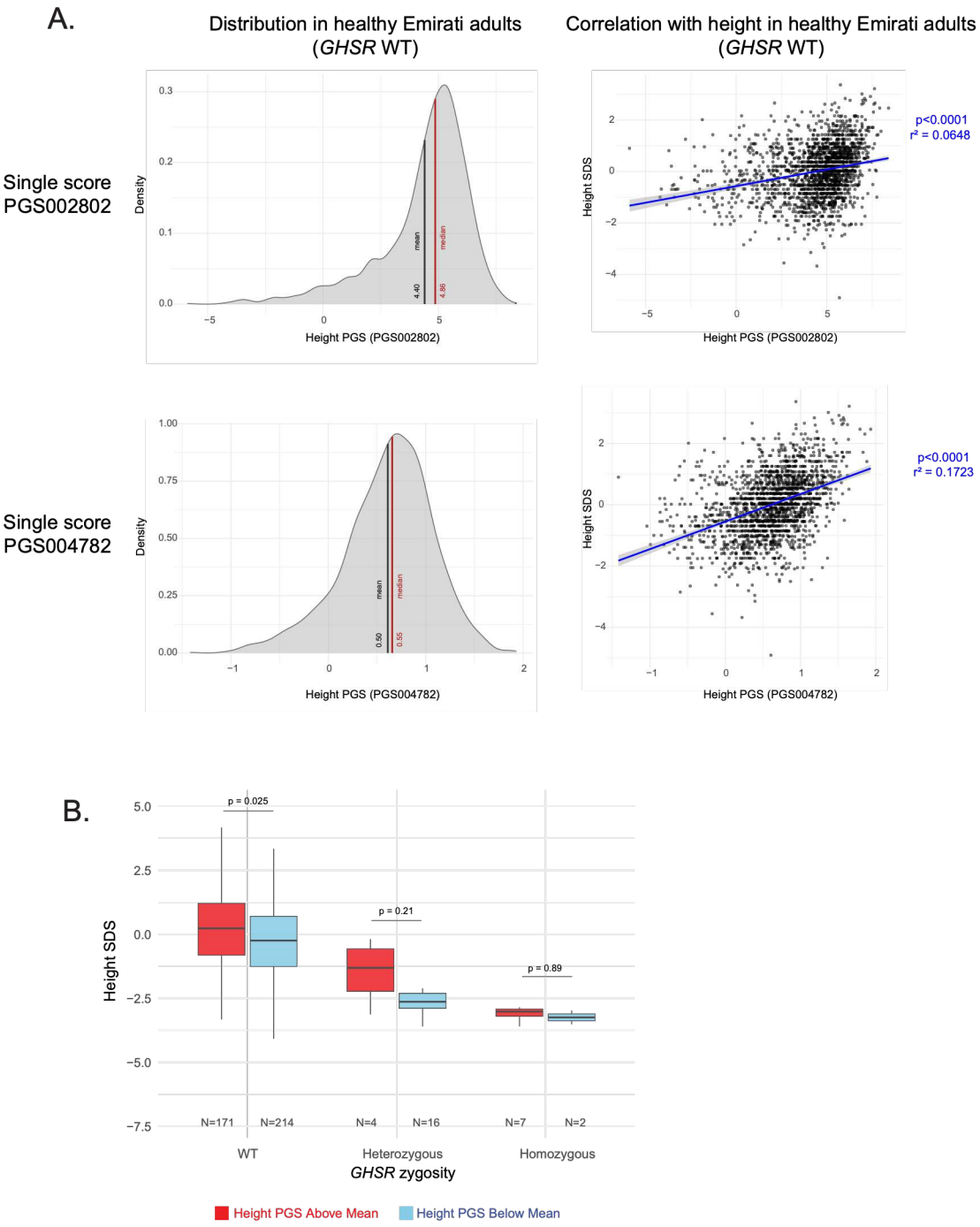
are standard errors over ten contiguous blocks and n = 1 trajectory per condition. Gα residues are numbered as in the deposited construct.

Dubai Health - Internal Use



Supplementary Figure 5. Effect of the *GHSR* Arg141Leu variant on locomotion in *C. elegans*. Representative one-minute locomotor tracks of *GHSR* wild-type, null, and Arg141Leu animals. Tracks were generated from 1-min video recordings using the TrackMate plugin in Fiji. The traces represent the trajectories of individual worms during the recording period; the scale bar indicates 1 mm.

Dubai Health - Internal Use



Supplementary Figure 6. A. Performance of two height polygenic scores (PGS) on height distribution within Emiratis. Distribution of two polygenic height scores within a healthy adult Emirati population with confirmed *GHSR* WT status and correlation of each with height SDS. The thick solid black line indicates the mean, while the red represents the median. **B.** Boxplot of height SDS of pediatric patients, stratified by height polygenic score grouping and

variant zygosity. Two-sided Wilcoxon rank-sum was run within each GHSR zygosity group and p values computed post-Benjamini–Hochberg (FDR) correction.

Supplementary Table 1. List of patients, along with their genetic and clinical information
Supplementary Table 2. Patient demographics
Supplementary Table 3. ACMG criteria applied for reclassification

Dubai Health - Internal Use

METHODS

Patient cohort

Pediatric patients with rare diseases were referred to the Dubai Health Genomic Medicine Center between January 2020 to May 2026. Genomic material was extracted and sequenced in a CAP-accredited clinical laboratory, as previously described [1,3–5]. Variants were classified according to the American College of Medical Genetics and Genomics and the Association for Molecular Pathology (ACMG/AMP) guidelines [126]. Clinical data was collected from patient records, including height, weight, bone age, biochemical testing, arginine stimulation testing, and imaging results, as well as from in-person and virtual genetic counseling and informed research consent sessions. Height deviation from target height was defined as the difference between the child's height SDS and mid-parental height SDS, using sex-specific population means and standard deviations of healthy Emirati adult men and women (**Supplementary Figure 1**), with negative values indicating heights below that expected from parental height. Response to GH treatment was assessed 7-25 months post-treatment initiation. Bone age SDS was calculated using Bonexpert V3.1. Short stature was defined as a height of at least 2 standard deviation scores (SDS) below the mean for age and gender. Growth hormone stimulation testing was performed using arginine according to the clinical protocol in use during the study period. A peak GH concentration <10 ng/mL represented the clinical diagnostic threshold used for GHD [10]. Clinical interpretation incorporated auxology, skeletal maturation, IGF-1/IGFBP-3 and imaging where available.

Patients were consented for the use of their genetic and clinical data for research. This study was approved by the Institutional Review Board at Mohammed Bin Rashid University (DAHC-MBRU-IRB-2023-002 and DAHC-MBRU-IRB-2025-21) and the Dubai Scientific Research Ethics Committee (DSREC), Dubai Health Authority (DSREC_EX_2026_060_01 and DSREC-05/2026_02).

Polygenic height score

We tested eight published height score models from the PGS Catalog (GRCh38-harmonised, computed from WGS) [11,12] and performance of each was evaluated by 10-fold cross-validation (out-of-fold R^2). The best-performing model (PGS004782) was tested on *GHSR* WT children (N=385), showing that those with low PGS had expectedly shorter stature compared to children with high PGS. Thus, we applied it on a subset of pediatric patients, carrying *GHSR* Arg141Leu variant, profiled by WGS (20 heterozygotes and 9 homozygotes).

Variant dating

Since the statistical phasing of rare alleles is challenging, we leveraged the fact that in homozygous samples, where both homologous chromosomes carry the putative founder

Dubai Health - Internal Use

allele, ancestral segments can be directly phased and defined by continuous runs of identical homozygous markers flanking the mutation. Any discordant marker (a heterozygous call or an opposite homozygote) signals the termination of ancestral sharing. We developed DASH [62] , a python script that extracts these ancestral tracts from multi-sample unphased VCF files and performs quality control. For homozygous individuals with the same mutation, the script identifies all informative markers flanking the mutation, walking outwards along both the upstream and downstream chromosome arms and evaluates continuous sharing across all individual pairs outwards from the mutation. A marker is concordant if a pair of individuals are homozygous for the same allele. The pairwise walk stops at the first run of consecutive discordant markers set by the user, with appropriate handling of technical sequencing artifacts and missing calls (see further options available in https://github.com/malmarri/DASH). Each individual's segment is then defined as the furthest coordinate (left and right independently) at which they still share with at least one partner. The age estimate is computed by implementing the analytical framework previously described [61].

Before running DASH, we then filtered the variants to ones found in the HGDP+1KG reference panel (MAF > 0.1%) and restricted to regions accessible to short-reads using the short-accessibility mask [127]. We then ran the script with the options: python3 dash.py --vcf <input.vcf.gz> --chrom chr3 --pos 172447992 --mask <mask.bed> --min-gq 20 --min-dp 10 --het-ab-alpha 0.01 --break-run 2 --merge-mismatch-bp 100 --genetic-map <genetic_map.map> --map-format plink --age-estimate --confidence 0.95 --plot <output_plot.pdf>.

Molecular dynamics simulations

Four all-atom systems were built from the active-state ghrelin-bound GHSR–Gq cryo-EM structure (PDB 7F9Y) [128] : WT and Arg141Leu receptors, each with and without ghrelin; the ghrelin-free systems were obtained by deleting the peptide from the assembled complex. ICL3 (receptor residues 242–256), absent from the map, was modeled and excluded from every analysis, and the variant was generated by replacing the Arg141 side chain before membrane building. Complexes were embedded in a POPC bilayer and solvated with TIP3P water [129] and 150 mM NaCl in CHARMM-GUI [130–132], giving approximately 238,000 atoms described by CHARMM36m and CHARMM36 [133] . After energy minimization and six-stage restrained equilibration, each system was simulated for 500 ns at 298.15 K and 1 bar in GROMACS version 2026.3 [134].

Cell culture

HEK293 cells (ECACC 85120602, confirmed by karyotyping and STR PCR analysis) were cultured in DMEM/F-12 (#31331, Gibco), 10% heat-inactivated fetal calf serum (FCS; Gibco)

Dubai Health - Internal Use

and 100 units/mL penicillin/100 µg/mL streptomycin (P/S; Gibco). Transfections were performed using Fugene HD (Promega) using a 1:3 DNA (µg):reagent (µL) ratio.

Plasmids

Bioluminescence resonance energy transfer (BRET) assays were performed to investigate GHSR expression levels, for which we used an expression plasmid encoding GHSR tagged at the C-terminus with NanoLuc luciferase (GHSR-NLuc) (provided by Dr C Gorvin, University of Birmingham, UK). Thereby, we used an mVenus-tagged CAAX motif derived from K-Ras (provided by Dr N Lambert, Augusta University, USA). For the calcium mobilization assay, a mitochondrial-targeted apo-aequorin (mtAEQ) expression plasmid was used (provided by Dr L Barak, Duke University Medical Center, USA). This assay, and all assays described below, used the pcDNA3.1(+)-GHSR (human) expression plasmid from the cDNA Resource Center (www.cdna.org) and its empty vector equivalent pcDNA3.1(+) as a carrier plasmid. To measure the SRE transcriptional activation, the SRE-luc2P vector (Promega plasmid #9PIE134) was utilized, combined with pRL-SV40 plasmid (Promega plasmid #TB550) to control for transfection efficiency. The CASE assay, used to measure $G\alpha_q$ subunit activation, utilized the Gq-CASE plasmid (gifted by Dr G Schulte; Addgene plasmid #168125; https://www.addgene.org/168125/; RRID: Addgene_168125). We performed ONE-GO assays to measure $G\alpha_{i2}$ subunit activation, for which we used the pLVX-CMV-Galpha-i2 ONE-GO plasmid (gifted by Dr M Garcia-Marcos; Addgene plasmid #189736; http://n2t.net/addgene:189736; RRID:Addgene_189736).

Site-directed mutagenesis was performed to generate the GHSR-R141L mutation in the GHSR expression plasmids GHSR-Nluc and pcDNA3.1-GHSR, using PfuTurbo DNA Polymerase (Agilent) with the following primers: GHSR forward GATGGCGAAGTAGAGCTCGACGCTC and reverse GAGCGTCGAGCTCTACTTCGCCATC primer. All constructs were verified using Sanger sequencing.

GHSR expression and localization

To measure GHSR expression levels and localization to the cell surface, we performed bystander BRET experiments using a modification of a previously described method [135]. Either wildtype or mutant GHSR-NLuc and mVenus-CAAX were co-transfected (50 ng each) with 400 ng pcDNA3.1 carrier vector using Fugene HD into 2.1×10^5 cells in suspension. Cells were then seeded into poly-D-lysine coated clear-bottom white 96-well plates at 3×10^4 cells/ well. After 48 h, the cells were washed with Hank's balanced salt solution (HBSS) (Gibco), which was then replaced with 50 µL/well of NanoBRET reagent (Promega; diluted 1:1,000 in HBSS). After ten minutes incubation, emission intensities were read at 450 ± 20 nm (NLuc luminescence) and 530 ± 20nm (mVenus fluorescence) in a CLARIOstar Plus plate reader (BMG LabTech). netBRET, a measure of cell surface receptor levels, was calculated

Dubai Health - Internal Use

using the formula ((fluorescence at 530 ± 20 nm/luminescence at 450 ± 20 nm)) - (background (fluorescence at 530 ± 20 nm/luminescence at 450 ± 20 nm)), with the background corresponding to the signal produced by cells expressing GHSR-NLuc alone under similar conditions. Total levels of GHSR expression were derived from the GHSR-NLuc luminescence signal directly, as described previously [136]. Results are shown as percentage of the wildtype GHSR.

Calcium mobilization

Mobilization of Ca^{2+} was measured by aequorin luminescence as described previously [136]. Briefly, 1.3×10^6 cells were seeded in T25 flasks. The next day, cells were transiently transfected with 2 µg mtAEQ, 50 ng of either wildtype or mutant pcDNA3.1- GHSR expression vector and 1 µg pcDNA3.1 as carrier using Fugene HD. After 48 h, the transfected cells were washed with PBS (Gibco) and harvested with PBS containing 5 mM Na_2EDTA (Sigma). Cells were resuspended in DMEM (Gibco; 31053), supplemented with 2 mM L-glutamine, 0.1% BSA (Sigma) and P/S. 1×10^6 cells/mL were incubated in 5 µM coelenterazine-h (Cayman) for 3 h on a roller bank at room temperature. Next, the cell suspension was diluted five-fold and incubated for 1 h. A three-fold dilution range of ghrelin (10 µM to 13.7 nM) was prepared in white-bottom 96-well plates. Immediately after injecting 1×10^4 cells in a well, the ghrelin response was measured as luminescent signal in a plate reader (CLARIOstar Plus, BMG LabTech). To account for the total activity of aequorin in the well, the remaining luminescence was measured upon lysis with 0.1% Triton X-100 (Sigma). The ghrelin response was corrected for total luminescence (i.e., the sum of both ghrelin and triton measurements), yielding the fractional response [137].

SRE transcriptional activity

Transcriptional activation downstream of the MAPK/ERK signaling pathway was determined using the SRE-luc2P vector. A mixture of 2 µg SRE-luc2P plasmid, 1 µg pRL-SV40 plasmid and 50 ng of either wildtype or mutant pcDNA3.1 (+)-GHSR was co-transfected into 3×10^5 cells using Fugene HD. These cell suspension transfections were plated into poly-D-lysine coated clear-bottom white 96-well plates at a density of 1.5×10^4 cells per well. After 24 h, cells were incubated overnight in serum starvation medium containing 0.2% charcoal-treated FCS. The next day, cells were incubated for 6 hours with a 10-fold dilution range of ghrelin (10 µM to 10 pM). Next, cells were lysed using a buffer containing 25 mM Tris-phosphate (pH= 7.8), 15% Glycerol, 1% Triton X-100, 1 mM DTT and 8 mM $MgCl_2$. The SRE response was measured using the Dual-Glo Luciferase Assay System according to the manufacturer's protocol (Promega) and calculated as relative firefly luciferase signal normalized to the *Renilla* luciferase signal.

Dubai Health - Internal Use

$G\alpha_q$ subunit activation

A $G\alpha_q$ BRET biosensor assay was used to measure $G\alpha_q$ subunit activation. A mixture of 500 ng Gq-CASE plasmid and 100 ng of either wildtype or mutant pcDNA3.1 (+)-GHSR or empty vector pcDNA3.1 was transfected into 6×10^5 cells in 1 mL suspension using Fugene HD. Cells were seeded at 3×10^4 cells per well in poly-D-lysine coated opaque white 96-well plates. After 48 h, cells were loaded with furimazine (Promega) in HBSS (Gibco). After two minutes, emission intensities were read at 450 ± 80 nm (NLuc luminescence) and 530 ± 30nm (mVenus fluorescence) in a CLARIOstar Plus plate reader (BMG LabTech). Next, 20 µL/well of ten-fold ghrelin dilutions (10 µM to 10 pM) were added and emission intensities were measured again. The BRET ratio (cpVenus/Nluc) declines upon activation of $G\alpha_q$. Calculated ΔBRET ratios were controlled for vehicle of the empty vector control. Inverse graphs were calculated as 1- ΔBRET.

$G\alpha_{i2}$ subunit activation

$G\alpha_{i2}$ subunit activation was measured using the ONE vector G-protein Optical (ONE-GO) biosensor plasmid. A mixture of 50 ng $G\alpha_{i2}$-ONE-GO, 50 ng of either wildtype or mutant pcDNA3.1 (+)-GHSR and 450 ng pGEM-3Zf(-) carrier plasmid (Promega) was transfected into 6×10^5 cells in suspension. Cells were seeded at 3×10^4 cells per well in poly-D-lysine coated opaque white 96-well plates. After 48 h, the cells were washed with HBSS. Next, cells were incubated with 80 µL/well of NanoBRET reagent (Promega; diluted 1:1,000 in HBSS) for two minutes, after which emission intensities were read at 450 ± 80 nm (NLuc luminescence) and 530 ± 30nm (mVenus fluorescence) in a CLARIOstar Plus plate reader (BMG LabTech). Next, 20 µL/well of ten-fold ghrelin dilutions (10 µM to 10 pM) were added and emission intensities were measured again. To quantify ligand-induced changes, ΔBRET ratios were calculated and controlled for each sample's vehicle control.

C. elegans culture and worm preparation

Wild-type (N2) and K03H6.5 null (tm4483) strains were obtained from the Caenorhabditis Genetics Center (CGC), University of Minnesota, USA, and the National BioResource Project (NBRP), Japan, respectively. For genotyping of the K03H6.5 null (tm4483) strain, the following primers were used: forward primer, 5'-CTGACAAGCCTTGCTCTCTG-3'; and reverse primer, 5'-GGTCCATTGGTGACCTAC-3'. The null strain represents a loss-of-function of K03H6.5, where a 407-bp deletion spanning exons 4 and 5 together with the flanking splice junctions, shifts the reading frame after residue 126 and introduces a premature stop codon, truncating the protein. The Arg141Leu strain [K03H6.5(syb11993)] was generated and Sanger sequenced by SunyBiotech Co., Ltd. The sgRNAs used were KO91-Sg1 (5'-CCCATTTCGATCATTGGACGTGC-3') and KO91-Sg2 (5'-CAAATTCCCATTTCGATCATTGG-3').

Dubai Health - Internal Use

The repair template was supplied as a donor sequence. Wild-type and mutant strains were cultured as described previously [138].

For synchronization, adult worms grown on seeded 6 cm NGM (nematode growth media) plates at 20°C were collected in M9 buffer and washed twice. Worms were pelleted at 6,000 × g for 1 min and resuspended in 1 mL freshly prepared alkaline hypochlorite solution (20% commercial bleach, 0.25 M NaOH). After gentle inversion for ~1 min to lyse adults, samples were centrifuged at 8,000 × g for 1 min. The bleach was immediately removed, and eggs were washed twice with M9 (12,000 × g for 1–2 min). Eggs were resuspended in residual M9 and transferred to fresh NGM plates for hatching at 15°C or 20°C. We collected synchronized worms at defined post-hatching stages: L1 (15 h), L2 (39 h), L3 (53 h), L4 (77 h), and 1-day adult (101 h) at 20°C for microscopy analysis.

Microscopy Analysis

An upright Leica DM6 B microscope equipped with an Andor iXon Ultra 897 EMCCD camera was used to acquire images at room temperature using Andor iQ 3.6.2 software. For body-length measurements, worms were immobilized with 10 mM levamisole, mounted on a fresh 2% agarose pad, and covered with a coverslip. Single-plane Differential Interference Contrast (DIC) images were acquired, and body length was measured using Andor software (version 3) by tracing the midline from the anterior tip of the head to the posterior tip of the tail. Folded, curled, or damaged worms were excluded from analysis. Subsequent image analysis was performed using ImageJ (NIH) or Fiji [139].

Mobility Assays

A Dino-Eye AM7025X Edge Series 5MP eyepiece camera was used to record worm movement for 1 min. Video recordings were analyzed using the TrackMate plugin in Fiji [140].

Dubai Health - Internal Use

References:

1. El Naofal, M. *et al.* The genomic landscape of rare disorders in the Middle East. *Genome Med.* **15**, 5 (2023).
2. Chekroun, I. *et al.* Genomics of rare diseases in the Greater Middle East. *Nat. Genet.* **57**, 505–514 (2025).
3. Alblooshi, K. *et al.* Citywide premarital genomic screening in a Middle Eastern population. *Nat. Med.* **32**, 1511–1518 (2026).
4. Halabi, N. *et al.* Rapid whole genome sequencing of critically ill pediatric patients from genetically underrepresented populations. *Genome Med.* **14**, 56 (2022).
5. Rabea, F. *et al.* Citywide implementation of a rapid whole-genome sequencing program for critically ill pediatric patients. *Nat. Med.* **32**, 3359–3371 (2026).
6. Seaver, L. H., Irons, M. & American College of Medical Genetics (ACMG) Professional Practice and Guidelines Committee. ACMG practice guideline: genetic evaluation of short stature. *Genet. Med.* **11**, 465–70 (2009).
7. Polidori, N., Castorani, V., Mohn, A. & Chiarelli, F. Deciphering short stature in children. *Ann. Pediatr. Endocrinol. Metab.* **25**, 69–79 (2020).
8. Dauber, A. *et al.* International guideline on genetic testing of children with short stature. *Eur. J. Endocrinol.* **194**, R17–R36 (2026).
9. Grimberg, A. *et al.* Guidelines for Growth Hormone and Insulin-Like Growth Factor-I Treatment in Children and Adolescents: Growth Hormone Deficiency, Idiopathic Short Stature, and Primary Insulin-Like Growth Factor-I Deficiency. *Horm. Res. Paediatr.* **86**, 361–397 (2016).
10. Collett-Solberg, P. F. *et al.* Diagnosis, Genetics, and Therapy of Short Stature in Children: A Growth Hormone Research Society International Perspective. *Horm. Res. Paediatr.* **92**, 1–14 (2019).
11. Truong, B. *et al.* Integrative polygenic risk score improves the prediction accuracy of complex traits and diseases. *Cell genomics* **4**, 100523 (2024).
12. Ma, Y., Patil, S., Zhou, X., Mukherjee, B. & Fritsche, L. G. ExPRSweb: An online repository with polygenic risk scores for common health-related exposures. *Am. J. Hum. Genet.* **109**, 1742–1760 (2022).
13. Yengo, L. *et al.* A saturated map of common genetic variants associated with human height. *Nature* **610**, 704–712 (2022).

Dubai Health - Internal Use

14. Jee, Y. H., Andrade, A. C., Baron, J. & Nilsson, O. Genetics of Short Stature. *Endocrinol. Metab. Clin. North Am.* **46**, 259–281 (2017).

15. Punt, L. D. *et al.* Loss-of-Function GHSR Variants Are Associated With Short Stature and Low IGF-I. *J. Clin. Endocrinol. Metab.* **110**, e1303–e1314 (2025).

16. Howard, A. D. *et al.* A receptor in pituitary and hypothalamus that functions in growth hormone release. *Science* **273**, 974–7 (1996).

17. Guan, X. M. *et al.* Distribution of mRNA encoding the growth hormone secretagogue receptor in brain and peripheral tissues. *Brain Res. Mol. Brain Res.* **48**, 23–9 (1997).

18. Sun, Y., Wang, P., Zheng, H. & Smith, R. G. Ghrelin stimulation of growth hormone release and appetite is mediated through the growth hormone secretagogue receptor. *Proc. Natl. Acad. Sci. U. S. A.* **101**, 4679–84 (2004).

19. Takaya, K. *et al.* Ghrelin strongly stimulates growth hormone release in humans. *J. Clin. Endocrinol. Metab.* **85**, 4908–11 (2000).

20. Wren, A. M. *et al.* The novel hypothalamic peptide ghrelin stimulates food intake and growth hormone secretion. *Endocrinology* **141**, 4325–8 (2000).

21. Kojima, M. *et al.* Ghrelin is a growth-hormone-releasing acylated peptide from stomach. *Nature* **402**, 656–60 (1999).

22. Holst, B., Cygankiewicz, A., Jensen, T. H., Ankersen, M. & Schwartz, T. W. High constitutive signaling of the ghrelin receptor--identification of a potent inverse agonist. *Mol. Endocrinol.* **17**, 2201–10 (2003).

23. Holst, B. *et al.* Common structural basis for constitutive activity of the ghrelin receptor family. *J. Biol. Chem.* **279**, 53806–17 (2004).

24. Pantel, J. *et al.* Recessive isolated growth hormone deficiency and mutations in the ghrelin receptor. *J. Clin. Endocrinol. Metab.* **94**, 4334–41 (2009).

25. Inoue, H. *et al.* Identification and functional analysis of novel human growth hormone secretagogue receptor (GHSR) gene mutations in Japanese subjects with short stature. *J. Clin. Endocrinol. Metab.* **96**, E373-8 (2011).

26. Pugliese-Pires, P. N. *et al.* Novel inactivating mutations in the GH secretagogue receptor gene in patients with constitutional delay of growth and puberty. *Eur. J. Endocrinol.* **165**, 233–41 (2011).

27. Riedl, S. *et al.* GH secretagogue receptor gene polymorphisms are associated with stature throughout childhood. *Eur. J. Endocrinol.* **166**, 1079–85 (2012).

Dubai Health - Internal Use

28. Wang, H.-J. *et al.* Ghrelin receptor gene: identification of several sequence variants in extremely obese children and adolescents, healthy normal-weight and underweight students, and children with short normal stature. *J. Clin. Endocrinol. Metab.* **89**, 157–62 (2004).

29. Pantel, J. *et al.* Loss of constitutive activity of the growth hormone secretagogue receptor in familial short stature. *J. Clin. Invest.* **116**, 760–8 (2006).

30. Barroso, P. S. *et al.* Clinical and Genetic Characterization of a Constitutional Delay of Growth and Puberty Cohort. *Neuroendocrinology* **110**, 959–966 (2020).

31. Jin, Q. *et al.* Novel SNPs of the caprine growth hormone secretagogue receptor (GHSR) gene and their association with growth traits in goats. *Biochem. Genet.* **48**, 847–56 (2010).

32. Zhang, B. *et al.* Effect of a single nucleotide polymorphism in the growth hormone secretagogue receptor (GHSR) gene on growth rate in pigs. *Gene* **634**, 68–73 (2017).

33. Torz, L. J. *et al.* Metabolic insights from a GHSR-A203E mutant mouse model. *Mol. Metab.* **39**, 101004 (2020).

34. Biagetti, B. *et al.* Contribution of Dynamic and Genetic Tests for Short Stature Diagnosing: A Case Report. *Diagnostics (Basel)* **13**, (2023).

35. Dimitri, P. *et al.* Opportunities for digitally-enabled personalization and decision support for pediatric growth hormone therapy. *Front. Endocrinol. (Lausanne).* **15**, 1436778 (2024).

36. Koledova, E., Tornincasa, V. & van Dommelen, P. Analysis of real-world data on growth hormone therapy adherence using a connected injection device. *BMC Med. Inform. Decis. Mak.* **20**, 176 (2020).

37. Kriström, B., Dahlgren, J., Niklasson, A., Nierop, A. F. M. & Albertsson-Wikland, K. The first-year growth response to growth hormone treatment predicts the long-term prepubertal growth response in children. *BMC Med. Inform. Decis. Mak.* **9**, 1 (2009).

38. Baş, F. *et al.* The distribution of exon 3-deleted/full-length growth hormone receptor polymorphism in the Turkish population. *J. Clin. Res. Pediatr. Endocrinol.* **3**, 126–31 (2011).

39. Kaabi, Y. A. Frequency of the exon 3-deleted/full-length growth hormone receptor polymorphism in Saudi Arabian population. *Saudi Med. J.* **38**, 1090–1095 (2017).

Dubai Health - Internal Use

40. Dos Santos, C. *et al.* A common polymorphism of the growth hormone receptor is associated with increased responsiveness to growth hormone. *Nat. Genet.* **36**, 720–4 (2004).

41. Filopanti, M. *et al.* The exon 3-deleted growth hormone receptor: molecular and functional characterization and impact on GH/IGF-I axis in physiological and pathological conditions. *J. Endocrinol. Invest.* **34**, 861–8 (2011).

42. Wassenaar, M. J. E. *et al.* Impact of the exon 3-deleted growth hormone (GH) receptor polymorphism on baseline height and the growth response to recombinant human GH therapy in GH-deficient (GHD) and non-GHD children with short stature: a systematic review and meta-analysis. *J. Clin. Endocrinol. Metab.* **94**, 3721–30 (2009).

43. Binder, G., Baur, F., Schweizer, R. & Ranke, M. B. The d3-growth hormone (GH) receptor polymorphism is associated with increased responsiveness to GH in Turner syndrome and short small-for-gestational-age children. *J. Clin. Endocrinol. Metab.* **91**, 659–64 (2006).

44. Rosenbaum, D. M., Rasmussen, S. G. F. & Kobilka, B. K. The structure and function of G-protein-coupled receptors. *Nature* **459**, 356–63 (2009).

45. Rovati, G. E., Capra, V. & Neubig, R. R. The highly conserved DRY motif of class A G protein-coupled receptors: beyond the ground state. *Mol. Pharmacol.* **71**, 959–64 (2007).

46. Gether, U. Uncovering molecular mechanisms involved in activation of G protein-coupled receptors. *Endocr. Rev.* **21**, 90–113 (2000).

47. Dohlman, H. G., Thorner, J., Caron, M. G. & Lefkowitz, R. J. Model systems for the study of seven-transmembrane-segment receptors. *Annu. Rev. Biochem.* **60**, 653–88 (1991).

48. Probst, W. C., Snyder, L. A., Schuster, D. I., Brosius, J. & Sealfon, S. C. Sequence alignment of the G-protein coupled receptor superfamily. *DNA Cell Biol.* **11**, 1–20 (1992).

49. Ioannidis, N. M. *et al.* REVEL: An Ensemble Method for Predicting the Pathogenicity of Rare Missense Variants. *Am. J. Hum. Genet.* **99**, 877–885 (2016).

50. Cheng, J. *et al.* Accurate proteome-wide missense variant effect prediction with AlphaMissense. *Science* **381**, eadg7492 (2023).

51. Cheng, J. *et al.* AlphaGenome Atlas: in silico mutagenesis of the entire human genome improves prioritization and interpretation of non-coding variants. *medRxiv* Preprint at https://doi.org/10.64898/2026.09.16.26363192 (2026).

52. Li, H.-Z. *et al.* The ghrelin receptor GHSR has two efficient agonists in the lobe-finned fish Latimeria chalumnae. *Biochem. Biophys. Res. Commun.* **679**, 110–115 (2023).

Dubai Health - Internal Use

53. Tine, M., Kuhl, H., Teske, P. R., Tschöp, M. H. & Jastroch, M. Diversification and coevolution of the ghrelin/growth hormone secretagogue receptor system in vertebrates. *Ecol. Evol.* **6**, 2516–35 (2016).

54. Kaiya, H. *et al.* Ghrelin Receptor in Two Species of Anuran Amphibian, Bullfrog (Rana catesbeiana), and Japanese Tree Frog (Hyla japonica). *Front. Endocrinol. (Lausanne).* **2**, 31 (2011).

55. Cai, W. *et al.* Sequence, genomic organization and expression of ghrelin receptor in grass carp, Ctenopharyngodon idellus. *Comp. Biochem. Physiol. A Mol. Integr. Physiol.* **179**, 54–61 (2015).

56. Lai, Z. *et al.* Evolutionary analysis of ghrelin in Actinopterygii. *Comp. Biochem. Physiol. Part D Genomics Proteomics* **56**, 101599 (2025).

57. Pir, M. S. *et al.* ConVarT: a search engine for matching human genetic variants with variants from non-human species. *Nucleic Acids Res.* **50**, D1172–D1178 (2022).

58. Fattahi, Z. *et al.* Iranome: A catalog of genomic variations in the Iranian population. *Hum. Mutat.* **40**, 1968–1984 (2019).

59. Koshy, R., Ranawat, A. & Scaria, V. al mena: a comprehensive resource of human genetic variants integrating genomes and exomes from Arab, Middle Eastern and North African populations. *J. Hum. Genet.* **62**, 889–894 (2017).

60. Vatsyayan, A. *et al.* DALIA- a comprehensive resource of Disease Alleles in Arab population. *PLoS One* **16**, e0244567 (2021).

61. Gandolfo, L. C., Bahlo, M. & Speed, T. P. Dating rare mutations from small samples with dense marker data. *Genetics* **197**, 1315–27 (2014).

62. Mohamed Almarri. DASH (Dating Ancestral Shared Haplotypes). Preprint at (2026).

63. Murray, P. G., Clayton, P. E. & Chernausek, S. D. A genetic approach to evaluation of short stature of undetermined cause. *Lancet Diabetes Endocrinol.* **6**, 564–574 (2018).

64. Al Jurayyan, N. A. M. Spectrum of endocrine disorders at the Paediatric Endocrine Clinic, King Khalid University Hospital, Riyadh, Kingdom of Saudi Arabia. *J. Taibah Univ. Med. Sci.* **7**, 99–103 (2012).

65. Martinez de Lapiscina, I. *et al.* Exome findings in children with short stature evaluated by growth hormone stimulation testing. *Eur. J. Endocrinol.* **194**, 285–297 (2026).

Dubai Health - Internal Use

66. Li, Q. *et al.* Molecular Diagnostic Yield of Exome Sequencing and Chromosomal Microarray in Short Stature: A Systematic Review and Meta-Analysis. *JAMA Pediatr.* **177**, 1149–1157 (2023).

67. Scalco, R. C. *et al.* Diagnostic yield of genetic testing in children with short stature: a systematic review. *Eur. J. Endocrinol.* **194**, S15–S24 (2026).

68. Yang, L. *et al.* Pathogenic gene screening in 91 Chinese patients with short stature of unknown etiology with a targeted next-generation sequencing panel. *BMC Med. Genet.* **19**, 212 (2018).

69. Ahn, J. *et al.* Next-generation sequencing-based mutational analysis of idiopathic short stature and isolated growth hormone deficiency in Korean pediatric patients. *Mol. Cell. Endocrinol.* **544**, 111489 (2022).

70. Scalco, R. C. *et al.* Diagnostic yield of genetic testing in children with short stature: a systematic review. *Eur. J. Endocrinol.* **194**, S15–S24 (2026).

71. Ammar, T. H. A. *et al.* Screening of GHSR, GHRHR, GH1 genes in isolated growth hormone deficiency disease in Egyptian patients. *Egyptian Journal of Medical Human Genetics* **25**, 16 (2024).

72. Fritez, N. *et al.* Molecular screening of a large cohort of Moroccan patients with congenital hypopituitarism. *Clin. Endocrinol. (Oxf).* **82**, 876–84 (2015).

73. Plachy, L. *et al.* Isolated growth hormone deficiency in children with vertically transmitted short stature: What do the genes tell us? *Front. Endocrinol. (Lausanne).* **13**, 1102968 (2022).

74. Damian, M. *et al.* Ghrelin receptor conformational dynamics regulate the transition from a preassembled to an active receptor:Gq complex. *Proc. Natl. Acad. Sci. U. S. A.* **112**, 1601–6 (2015).

75. Kohno, D., Gao, H.-Z., Muroya, S., Kikuyama, S. & Yada, T. Ghrelin directly interacts with neuropeptide-Y-containing neurons in the rat arcuate nucleus: Ca2+ signaling via protein kinase A and N-type channel-dependent mechanisms and cross-talk with leptin and orexin. *Diabetes* **52**, 948–56 (2003).

76. Acharya, S. & Karnik, S. S. Modulation of GDP release from transducin by the conserved Glu134-Arg135 sequence in rhodopsin. *J. Biol. Chem.* **271**, 25406–11 (1996).

77. Weis, W. I. & Kobilka, B. K. The Molecular Basis of G Protein-Coupled Receptor Activation. *Annu. Rev. Biochem.* **87**, 897–919 (2018).

Dubai Health - Internal Use

78. Vogel, R. *et al.* Functional role of the 'ionic lock'--an interhelical hydrogen-bond network in family A heptahelical receptors. *J. Mol. Biol.* **380**, 648–55 (2008).

79. Palczewski, K. *et al.* Crystal structure of rhodopsin: A G protein-coupled receptor. *Science* **289**, 739–45 (2000).

80. Ballesteros, J. A. *et al.* Activation of the beta 2-adrenergic receptor involves disruption of an ionic lock between the cytoplasmic ends of transmembrane segments 3 and 6. *J. Biol. Chem.* **276**, 29171–7 (2001).

81. Scheer, A., Fanelli, F., Costa, T., De Benedetti, P. G. & Cotecchia, S. Constitutively active mutants of the alpha 1B-adrenergic receptor: role of highly conserved polar amino acids in receptor activation. *EMBO J.* **15**, 3566–78 (1996).

82. Zhu, S. Z., Wang, S. Z., Hu, J. & el-Fakahany, E. E. An arginine residue conserved in most G protein-coupled receptors is essential for the function of the m1 muscarinic receptor. *Mol. Pharmacol.* **45**, 517–23 (1994).

83. Alewijnse, A. E. *et al.* The effect of mutations in the DRY motif on the constitutive activity and structural instability of the histamine H(2) receptor. *Mol. Pharmacol.* **57**, 890–8 (2000).

84. Gáborik, Z. *et al.* The Role of a Conserved Region of the Second Intracellular Loop in AT1 Angiotensin Receptor Activation and Signaling. *Endocrinology* **144**, 2220–2228 (2003).

85. Arora, K. K., Cheng, Z. & Catt, K. J. Mutations of the conserved DRS motif in the second intracellular loop of the gonadotropin-releasing hormone receptor affect expression, activation, and internalization. *Mol. Endocrinol.* **11**, 1203–12 (1997).

86. Gyombolai, P., Tóth, A. D., Tímár, D., Turu, G. & Hunyady, L. Mutations in the 'DRY' motif of the CB1 cannabinoid receptor result in biased receptor variants. *J. Mol. Endocrinol.* **54**, 75–89 (2015).

87. Lu, Z. L., Curtis, C. A., Jones, P. G., Pavia, J. & Hulme, E. C. The role of the aspartate-arginine-tyrosine triad in the m1 muscarinic receptor: mutations of aspartate 122 and tyrosine 124 decrease receptor expression but do not abolish signaling. *Mol. Pharmacol.* **51**, 234–41 (1997).

88. Capra, V. *et al.* Mutational analysis of the highly conserved ERY motif of the thromboxane A2 receptor: alternative role in G protein-coupled receptor signaling. *Mol. Pharmacol.* **66**, 880–9 (2004).

Dubai Health - Internal Use

89. Franke, R. R., Sakmar, T. P., Graham, R. M. & Khorana, H. G. Structure and function in rhodopsin. Studies of the interaction between the rhodopsin cytoplasmic domain and transducin. *J. Biol. Chem.* **267**, 14767–74 (1992).

90. Schöneberg, T. *et al.* V2 vasopressin receptor dysfunction in nephrogenic diabetes insipidus caused by different molecular mechanisms. *Hum. Mutat.* **12**, 196–205 (1998).

91. Rhee, M.-H., Nevo, I., Levy, R. & Vogel, Z. Role of the highly conserved Asp-Arg-Tyr motif in signal transduction of the CB2 cannabinoid receptor. *FEBS Lett.* **466**, 300–304 (2000).

92. Wilbanks, A. M., Laporte, S. A., Bohn, L. M., Barak, L. S. & Caron, M. G. Apparent loss-of-function mutant GPCRs revealed as constitutively desensitized receptors. *Biochemistry* **41**, 11981–9 (2002).

93. Seibold A, D. M. B. M. Mutations of the DRY motif that preserve beta 2-adrenoceptor coupling. *Recept channels* **5**, 375–385 (1998).

94. Scheer, A. *et al.* Mutational analysis of the highly conserved arginine within the Glu/Asp-Arg-Tyr motif of the alpha(1b)-adrenergic receptor: effects on receptor isomerization and activation. *Mol. Pharmacol.* **57**, 219–31 (2000).

95. Rovati, G. E., Capra, V. & Neubig, R. R. The highly conserved DRY motif of class A G protein-coupled receptors: beyond the ground state. *Mol. Pharmacol.* **71**, 959–64 (2007).

96. Auger, G. A., Pease, J. E., Shen, X., Xanthou, G. & Barker, M. D. Alanine scanning mutagenesis of CCR3 reveals that the three intracellular loops are essential for functional receptor expression. *Eur. J. Immunol.* **32**, 1052–8 (2002).

97. Jones, P. G., Curtis, C. A. & Hulme, E. C. The function of a highly-conserved arginine residue in activation of the muscarinic M1 receptor. *Eur. J. Pharmacol.* **288**, 251–7 (1995).

98. Min, K. C., Zvyaga, T. A., Cypess, A. M. & Sakmar, T. P. Characterization of mutant rhodopsins responsible for autosomal dominant retinitis pigmentosa. Mutations on the cytoplasmic surface affect transducin activation. *J. Biol. Chem.* **268**, 9400–4 (1993).

99. Iannaccone, A. *et al.* Retinitis pigmentosa associated with rhodopsin mutations: Correlation between phenotypic variability and molecular effects. *Vision Res.* **46**, 4556–67 (2006).

100. Andréasson, S., Ehinger, B., Abrahamson, M. & Fex, G. A six-generation family with autosomal dominant retinitis pigmentosa and a rhodopsin gene mutation. *Ophthalmic Paediatr. Genet.* **13**, 145–153 (1992).

Dubai Health - Internal Use

101. Feldman, B. J. *et al.* Nephrogenic syndrome of inappropriate antidiuresis. *N. Engl. J. Med.* **352**, 1884–90 (2005).

102. Silventoinen, K. Determinants of variation in adult body height. *J. Biosoc. Sci.* **35**, 263–85 (2003).

103. Abdulrazzaq, Y. M., Aburawi, E., Abdulrahman, M., Alshamsi, A. & Zidan, M. Reference growth charts for height and weight, for the UAE, the UAEMCGS 2 study. *Ann. Hum. Biol.* **51**, 2437167 (2024).

104. Ali, H., Alahmad, B., Abu-Farha, M., Abubaker, J. & Al-Mulla, F. The evolutionary basis for type 2 diabetes prevalence in the Arabian Peninsula. *Lancet Diabetes Endocrinol.* **13**, 998–999 (2025).

105. Hofmeister, R. J. *et al.* Parent-of-origin effects on complex traits in up to 236,781 individuals. *Nature* **646**, 647–656 (2025).

106. Benonisdottir, S. *et al.* Epigenetic and genetic components of height regulation. *Nat. Commun.* **7**, 13490 (2016).

107. Zoledziewska, M. *et al.* Height-reducing variants and selection for short stature in Sardinia. *Nat. Genet.* **47**, 1352–1356 (2015).

108. Yang, J. *et al.* Common SNPs explain a large proportion of the heritability for human height. *Nat. Genet.* **42**, 565–9 (2010).

109. Fahed, A. C. *et al.* Polygenic background modifies penetrance of monogenic variants for tier 1 genomic conditions. *Nat. Commun.* **11**, 3635 (2020).

110. Badaru, A. & Wilson, D. M. Alternatives to growth hormone stimulation testing in children. *Trends Endocrinol. Metab.* **15**, 252–8 (2004).

111. Tenenbaum-Rakover, Y. *et al.* Can auxology, IGF-I and IGFBP-3 measurements followed by MRI and genetic tests replace GH stimulation tests in the diagnosis of GH deficiency in children? *J. Pediatr. Endocrinol. Metab.* **23**, 387–94 (2010).

112. Obara-Moszyńska, M., Kedzia, A., Korman, E. & Niedziela, M. Usefulness of growth hormone (GH) stimulation tests and IGF-I concentration measurement in GH deficiency diagnosis. *J. Pediatr. Endocrinol. Metab.* **21**, 569–79 (2008).

113. Obara-Moszyńska, M., Kedzia, A., Korman, E. & Niedziela, M. Usefulness of growth hormone (GH) stimulation tests and IGF-I concentration measurement in GH deficiency diagnosis. *J. Pediatr. Endocrinol. Metab.* **21**, 569–79 (2008).

Dubai Health - Internal Use

114. Giannakopoulos, A., Kallimani, E., Efthymiadou, A. & Chrysis, D. Growth Hormone Treatment Response: Associated Factors and Stimulated Growth Hormone Secretion Indices in Prepubertal Children with Idiopathic GH Deficiency. *Exp. Clin. Endocrinol. Diabetes* **133**, 34–39 (2025).

115. Pozzobon, G. *et al.* Growth hormone therapy in children: predictive factors and short-term and long-term response criteria. *Endocrine* **66**, 614–621 (2019).

116. Cammisa, I., De Fortuna, G., Rulli, E., Rigante, D. & Cipolla, C. Predictors of Response to Growth Hormone Therapy in Children with Idiopathic Growth Hormone Deficiency: A Narrative Review. *Children (Basel)* **13**, (2026).

117. Blethen, S. L. *et al.* Factors predicting the response to growth hormone (GH) therapy in prepubertal children with GH deficiency. *J. Clin. Endocrinol. Metab.* **76**, 574–9 (1993).

118. Katritch, V., Cherezov, V. & Stevens, R. C. Diversity and modularity of G protein-coupled receptor structures. *Trends Pharmacol. Sci.* **33**, 17–27 (2012).

119. Zhang, M. *et al.* G protein-coupled receptors (GPCRs): advances in structures, mechanisms, and drug discovery. *Signal Transduct. Target. Ther.* **9**, 88 (2024).

120. Takeda, S., Kadowaki, S., Haga, T., Takaesu, H. & Mitaku, S. Identification of G protein-coupled receptor genes from the human genome sequence. *FEBS Lett.* **520**, 97–101 (2002).

121. Herrera, L. P. T. *et al.* GPCRdb in 2025: adding odorant receptors, data mapper, structure similarity search and models of physiological ligand complexes. *Nucleic Acids Res.* **53**, D425–D435 (2025).

122. Sautel, M. & Milligan, G. Molecular manipulation of G-protein-coupled receptors: a new avenue into drug discovery. *Curr. Med. Chem.* **7**, 889–96 (2000).

123. Sriram, K. & Insel, P. A. G Protein-Coupled Receptors as Targets for Approved Drugs: How Many Targets and How Many Drugs? *Mol. Pharmacol.* **93**, 251–258 (2018).

124. Schröer, S. & Seifert, R. Do GPCRs constitute the target of 30% of newly approved drugs in Germany? *Naunyn. Schmiedebergs. Arch. Pharmacol.* **399**, 5575–5604 (2026).

125. Hopkins, A. L. & Groom, C. R. The druggable genome. *Nat. Rev. Drug Discov.* **1**, 727–30 (2002).

126. Richards, S. *et al.* Standards and guidelines for the interpretation of sequence variants: a joint consensus recommendation of the American College of Medical Genetics and Genomics and the Association for Molecular Pathology. *Genet. Med.* **17**, 405–24 (2015).

Dubai Health - Internal Use

127. Bergström, A. *et al.* Insights into human genetic variation and population history from 929 diverse genomes. *Science* **367**, (2020).

128. Wang, Y. *et al.* Molecular recognition of an acyl-peptide hormone and activation of ghrelin receptor. *Nat. Commun.* **12**, 5064 (2021).

129. Jorgensen, W. L., Chandrasekhar, J., Madura, J. D., Impey, R. W. & Klein, M. L. Comparison of simple potential functions for simulating liquid water. *J. Chem. Phys.* **79**, 926–935 (1983).

130. Jo, S., Kim, T., Iyer, V. G. & Im, W. CHARMM-GUI: a web-based graphical user interface for CHARMM. *J. Comput. Chem.* **29**, 1859–65 (2008).

131. Wu, E. L. *et al.* CHARMM-GUI Membrane Builder toward realistic biological membrane simulations. *J. Comput. Chem.* **35**, 1997–2004 (2014).

132. Lee, J. *et al.* CHARMM-GUI Input Generator for NAMD, GROMACS, AMBER, OpenMM, and CHARMM/OpenMM Simulations Using the CHARMM36 Additive Force Field. *J. Chem. Theory Comput.* **12**, 405–13 (2016).

133. Huang, J. *et al.* CHARMM36m: an improved force field for folded and intrinsically disordered proteins. *Nat. Methods* **14**, 71–73 (2017).

134. Abraham, M. J. *et al.* GROMACS: High performance molecular simulations through multi-level parallelism from laptops to supercomputers. *SoftwareX* **1–2**, 19–25 (2015).

135. Wan, Q. *et al.* Mini G protein probes for active G protein-coupled receptors (GPCRs) in live cells. *J. Biol. Chem.* **293**, 7466–7473 (2018).

136. Prins, K. *et al.* Syndecans modulate ghrelin receptor signaling. *J. Mol. Endocrinol.* **74**, (2025).

137. Delhanty, P. J. D. *et al.* Unsaturated fatty acids prevent desensitization of the human growth hormone secretagogue receptor by blocking its internalization. *Am. J. Physiol. Endocrinol. Metab.* **299**, E497-505 (2010).

138. Brenner, S. The genetics of Caenorhabditis elegans. *Genetics* **77**, 71–94 (1974).

139. Schneider, C. A., Rasband, W. S. & Eliceiri, K. W. NIH Image to ImageJ: 25 years of image analysis. *Nat. Methods* **9**, 671–5 (2012).

140. Tinevez, J.-Y. *et al.* TrackMate: An open and extensible platform for single-particle tracking. *Methods* **115**, 80–90 (2017).

Dubai Health - Internal Use

Supplementary Files

This is a list of supplementary files associated with this preprint. Click to download.

- SupplementaryTables.xlsx